Overview of Computer Simulation Methods Used to Study and Design New Materials: Examples from the Study of Solid Electrolytes*

N. A. W. Holzwarth**

Department of Physics

Wake Forest University, Winston-Salem, NC, USA, 27109

*Supported by NSF Grant DMR-1105485 and WFU's Center for Energy, Environment, and Sustainability.

**With help from: Nicholas Lepley, Ahmad Al-Qawasmeh, Jason Howard, and Larry Rush (physics graduate students), Yaojun Du (previous physics postdoc) and colleagues from WFU chemistry department – Dr. Keerthi Senevirathne, Dr. Cynthia Day, Professor Michael Gross, Professor Abdessadek Lachgar, and Zachary Hood (currently at ORNL)

WAKE FOREST UNIVERSITY

Outline

- Overview of computational methods
  - What is meant by “first principles”?
  - Evaluation of computational results and comparison with reality
- Why are we interested in solid electrolytes?
- How can computer simulations help?
  - Survey of known solid electrolytes
  - Prediction of new solid electrolytes
  - Study of electrolyte/electrode interfaces
- Remaining challenges

- **What is meant by "first principles" simulation methods?**

  A series of well-controlled approximations

Summary of "first-principles" calculation methods

Exact Schrödinger equation:

Electronic coordinates

Atomic coordinates

$$\mathcal{H}(\{\mathbf{r}_i\},\{\mathbf{R}^a\})\Psi_\alpha(\{\mathbf{r}_i\},\{\mathbf{R}^a\}) = E_\alpha \Psi_\alpha(\{\mathbf{r}_i\},\{\mathbf{R}^a\})$$

where

$$\mathcal{H}(\{\mathbf{r}_i\},\{\mathbf{R}^a\}) = \mathcal{H}^{\text{Nuclei}}(\{\mathbf{R}^a\}) + \mathcal{H}^{\text{Electrons}}(\{\mathbf{r}_i\},\{\mathbf{R}^a\})$$

Born-Oppenheimer approximation

Born & Huang, **Dynamical Theory of Crystal Lattices**, Oxford (1954)

Approximate factorization:

$$\Psi_\alpha(\{\mathbf{r}_i\},\{\mathbf{R}^a\}) = X_\alpha^{\text{Nuclei}}(\{\mathbf{R}^a\})\Upsilon_\alpha^{\text{Electrons}}(\{\mathbf{r}_i\},\{\mathbf{R}^a\})$$

Summary of "first-principles" calculation methods -- continued

Electronic Schrödinger equation:

$$\mathcal{H}^{\text{Electrons}}(\{\mathbf{r}_i\},\{\mathbf{R}^a\})\Upsilon_\alpha^{\text{Electrons}}(\{\mathbf{r}_i\},\{\mathbf{R}^a\}) = U_\alpha(\{\mathbf{R}^a\})\Upsilon_\alpha^{\text{Electrons}}(\{\mathbf{r}_i\},\{\mathbf{R}^a\})$$

$$\mathcal{H}^{\text{Electrons}}(\{\mathbf{r}_i\},\{\mathbf{R}^a\}) = -\frac{\hbar^2}{2m}\sum_i \nabla_i^2 - \sum_{a,i}\frac{Z^a e^2}{|\mathbf{r}_i - \mathbf{R}^a|} + \sum_{i<j}\frac{e^2}{|\mathbf{r}_i - \mathbf{r}_j|}$$

Density functional theory

Hohenberg and Kohn, *Phys. Rev*. **136** B864 (1964)

Kohn and Sham, *Phys. Rev*. **140** A1133 (1965)

For electronic ground state: $\alpha \Rightarrow 0$

Mean field approximation: $U_0(\{\mathbf{R}^a\}) \Rightarrow U_0(\{\rho(\mathbf{r})\},\{\mathbf{R}^a\})$

Electron density

$$\mathcal{H}_{\text{KS}}^{\text{Electrons}}(\mathbf{r},\rho(\mathbf{r}),\{\mathbf{R}^a\})\psi_n(\mathbf{r}) = \varepsilon_n\psi_n(\mathbf{r}) \qquad \rho(\mathbf{r}) = \sum_n |\psi_n(\mathbf{r})|^2$$

Independent electron wavefunction

Summary of "first-principles" calculation methods -- continued

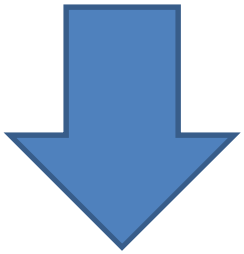

Nuclear Hamiltonian (usually treated classically)

$$\mathcal{H}^{\text{Nuclei}}\left(\{\mathbf{R}^a\}\right) = \sum_a \frac{\mathbf{P}^{a2}}{2M^a} + U_0(\{\rho(\mathbf{r})\},\{\mathbf{R}^a\})$$

Electron density

More computational details:

$$\mathcal{H}_{\mathrm{KS}}^{\mathrm{Electrons}}(\mathbf{r},\rho(\mathbf{r}),\{\mathbf{R}^a\}) = -\frac{\hbar^2\nabla^2}{2m} + \sum_a \frac{-Z^a e^2}{|\mathbf{r}-\mathbf{R}^a|} + e^2\int d^3r' \frac{\rho(\mathbf{r}')}{|\mathbf{r}-\mathbf{r}'|} + V_{xc}\left(\rho(\mathbf{r})\right)$$

electron-nucleus | electron-electron | exchange-correlation

Exchange-correlation functionals:

- LDA: J. Perdew and Y. Wang, Phys. Rev. B **45**, 13244 (1992)
- GGA: J. Perdew, K. Burke, and M. Ernzerhof, PRL **77**, 3865 (1996)
- HSE06: J. Heyd, G. E. Scuseria, and M. Ernzerhof, JCP **118**, 8207 (2003)

Numerical methods:

- "Muffin-tin" construction: Augmented Plane Wave developed by Slater → "linearized" version by Andersen:
  - J. C. Slater, Phys. Rev. **51** 846 (1937)
  - O. K. Andersen, Phys. Rev. B **12** 3060 (1975) (LAPW)
- Pseudopotential methods:
  - J. C. Phillips and L. Kleinman, Phys. Rev. **116** 287 (1959) -- original idea
  - P. Blöchl, Phys. Rev. B. 50 17953 (1994) – Projector Augmented Wave (PAW) method

Outputs of calculations:

Ground state energy:

$U_0(\{\rho(\mathbf{r})\},\{\mathbf{R}^a\})$ $\Rightarrow$ Determine formation energies

$\min|_{\{\mathbf{R}^a\}}\left(U_0(\{\rho(\mathbf{r})\},\{\mathbf{R}^a\})\right)$ $\Rightarrow$ Determine structural parameters

$\Rightarrow$ Stable and meta-stable structures

$\Rightarrow$ Normal modes of vibration

$\rho(\mathbf{r})=\sum_n|\psi_n(\mathbf{r})|^2$ $\Rightarrow$ Self-consistent electron density

$\{\varepsilon_n\}$ $\Rightarrow$ One-electron energies; densities of states

Public domain codes available for electronic structure calculations

Method	Codes	Comments
LAPW	www.wien2k.at elk.sourceforge.net	Works well for smaller unit cells; variable unit cell optimization not implemented. Need to choose non-overlapping muffin tin radii and avoid "ghost" solutions.
PAW	www.abinit.org www.quantum-espresso.org	Works well for large unit cells (<200 atoms or so); includes variable unit cell optimization.
ATOMPAW	pwpaw.wfu.edu	Generates PAW datasets for *abinit* and *quantum-espresso* (and other codes)

Other efforts:

- Gerbrand Ceder's group at MIT – Materials Project; A Materials Genome Approach -- http://www.materialsproject.org/
- Stefano Curtarolo's group at Duke – Energy Materials Laboratory -- http://materials.duke.edu/

ATOMPAW Code for generating atomic datasets for PAW calculations

Holzwarth, Tackett, and Matthews, CPC 135 329 (2001) http://pwpaw.wfu.edu

ATOMPAW
INFO
DATASETS
CONTRIBUTERS
CONTACT INFO
NAWH Web
PHYSICS Web
WFU Web

ATOMPAW

Download source code and example files:

- atompaw-4.0.0.12.tar.gz (5.4mb) 12/23/2014: Slight update of new version of atompaw code. In additon to previous updates, added PBESOL output for Quantum Espresso interface and added interface for SOCORRO.
- atompaw-3.1.0.3.tar.gz (3.8mb) Updated version of *atompaw* code (01/03/2014 and 09/18/2013 -- Marc Torrent and Francois Jollet introduced improvements to the XML and abinit dataset generation routines; 07/09/2013 -- Marc Torrent introduced small corrections; 06/22/2013 -- Marc Torrent and Francois Jollet added a new option for outputting a file in XML format according to the specifications set up by the GPAW group . The output file format is controled by a menu at

"Small Core" Datasets for PAW Functions

1 H																2 He
3 Li	4 Be											5 B	6 C	7 N	8 O	9 F	10 Ne
11 Na	12 Mg											13 Al	14 Si	15 P	16 S	17 Cl	18 Ar
19 K	20 Ca	21 Sc	22 Ti	23 V	24 Cr	25 Mn	26 Fe	27 Co	28 Ni	29 Cu	30 Zn	31 Ga	32 Ge	33 As	34 Se	35 Br	36 Kr
37 Rb	38 Sr	39 Y	40 Zr	41 Nb	42 Mo	43 Tc	44 Ru	45 Rh	46 Pd	47 Ag	48 Cd	49 In	50 Sn	51 Sb	52 Te	53 I	54 Xe
55 Cs	56 Ba		72 Hf	73 Ta	74 W	75 Re	76 Os	77 Ir	78 Pt	79 Au	80 Hg	81 Tl	82 Pb	83 Bi	84 Po	85 At	86 Rn

"Large Core" Datasets for PAW Functions

1 H																2 He
3 Li	4 Be											5 B	6 C	7 N	8 O	9 F	10 Ne
11 Na	12 Mg											13 Al	14 Si	15 P	16 S	17 Cl	18 Ar
19 K	20 Ca	21 Sc	22 Ti	23 V	24 Cr	25 Mn	26 Fe	27 Co	28 Ni	29 Cu	30 Zn	31 Ga	32 Ge	33 As	34 Se	35 Br	36 Kr
37 Rb	38 Sr	39 Y	40 Zr	41 Nb	42 Mo	43 Tc	44 Ru	45 Rh	46 Pd	47 Ag	48 Cd	49 In	50 Sn	51 Sb	52 Te	53 I	54 Xe
55 Cs	56 Ba		72 Hf	73 Ta	74 W	75 Re	76 Os	77 Ir	78 Pt	79 Au	80 Hg	81 Tl	82 Pb	83 Bi	84 Po	85 At	86 Rn

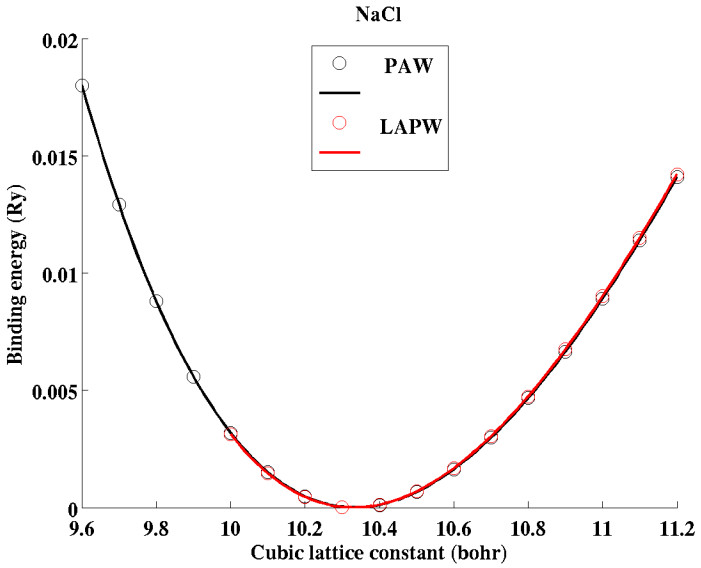

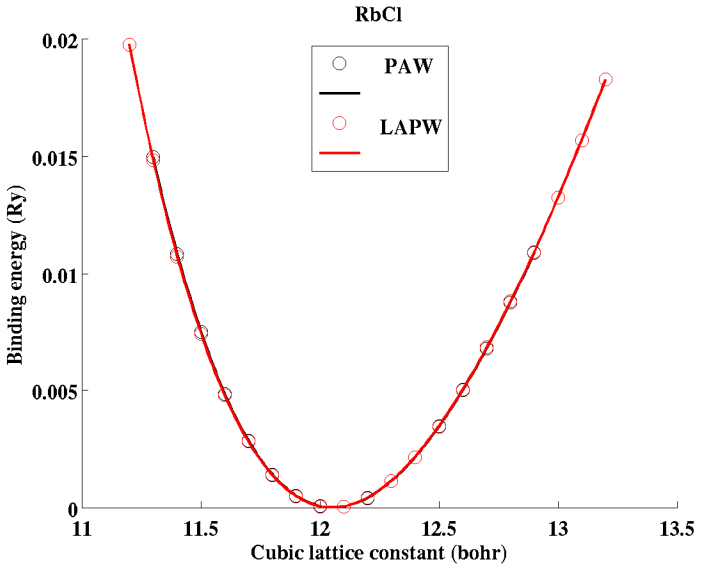

- **What do computer simulations have to do with reality?**

Example comparison of computational results with experimental measurements --

Li_3PO_4 crystals

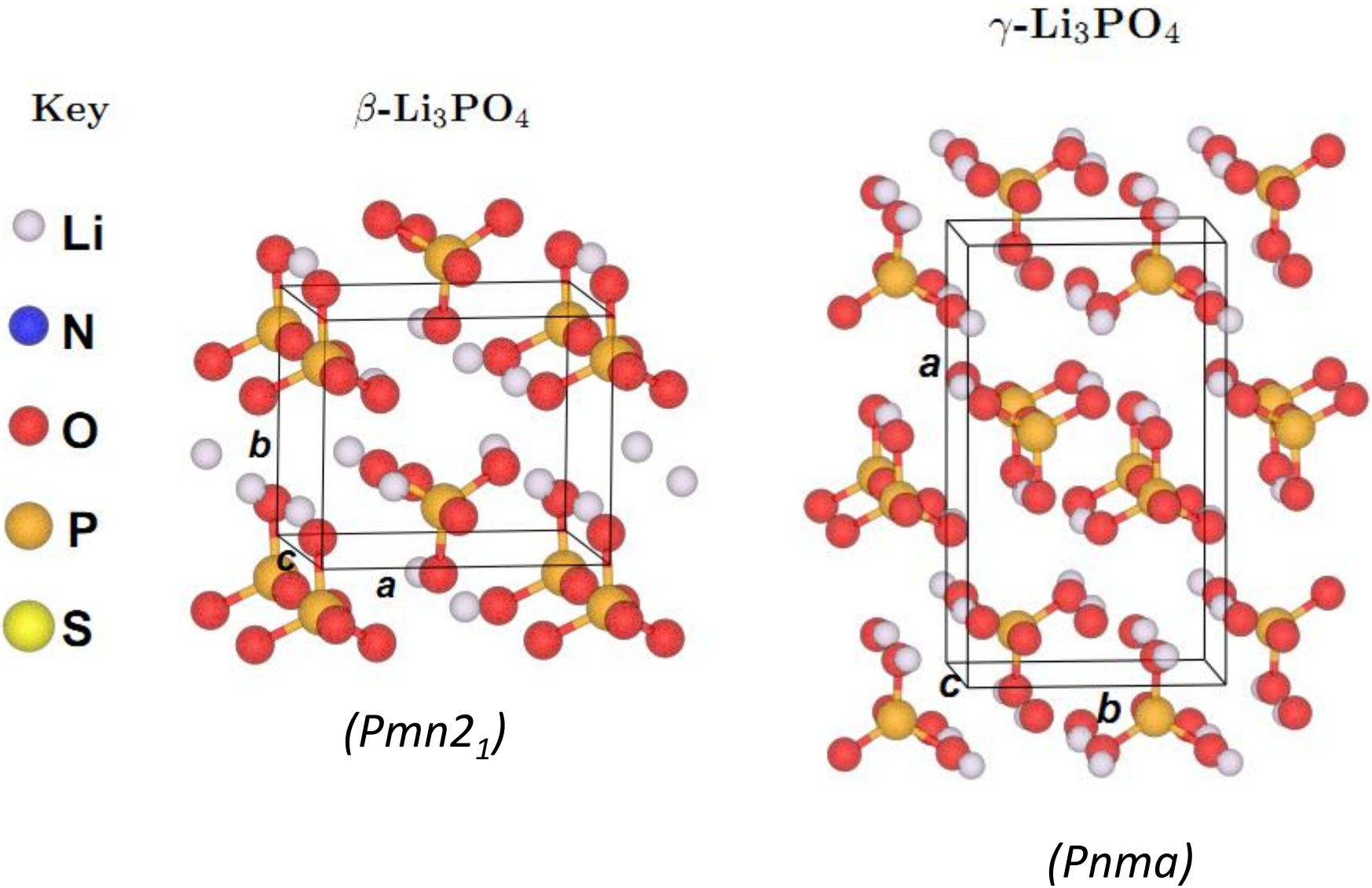

(Pmn2$_1$)

(Pnma)

Validation of calculations

Raman spectra – Experiment & Calculation

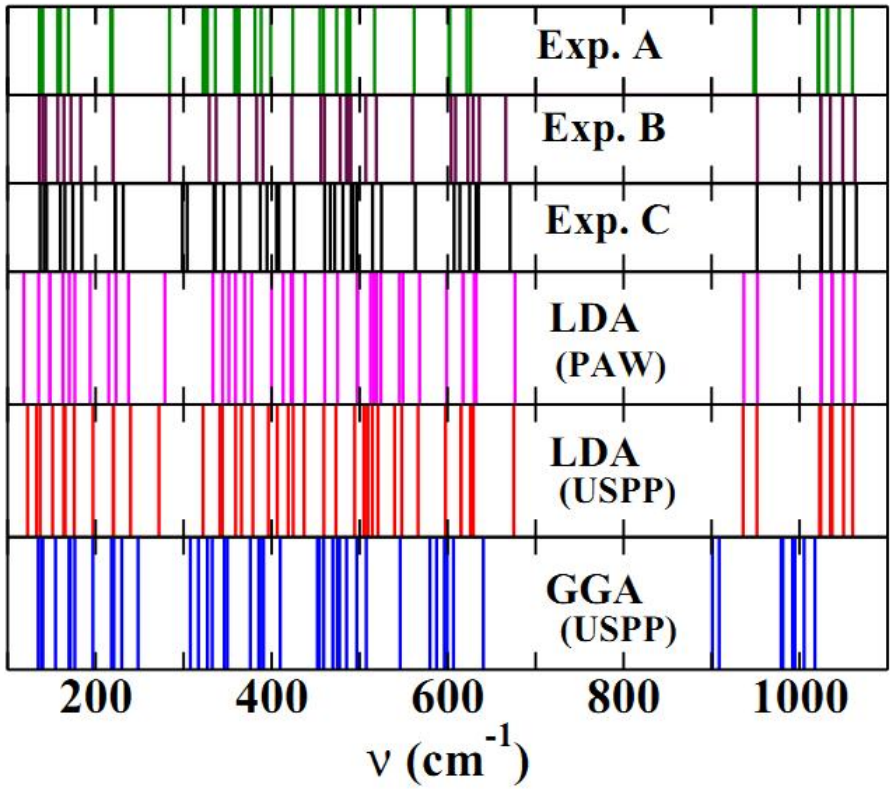

γ-Li_3PO_4

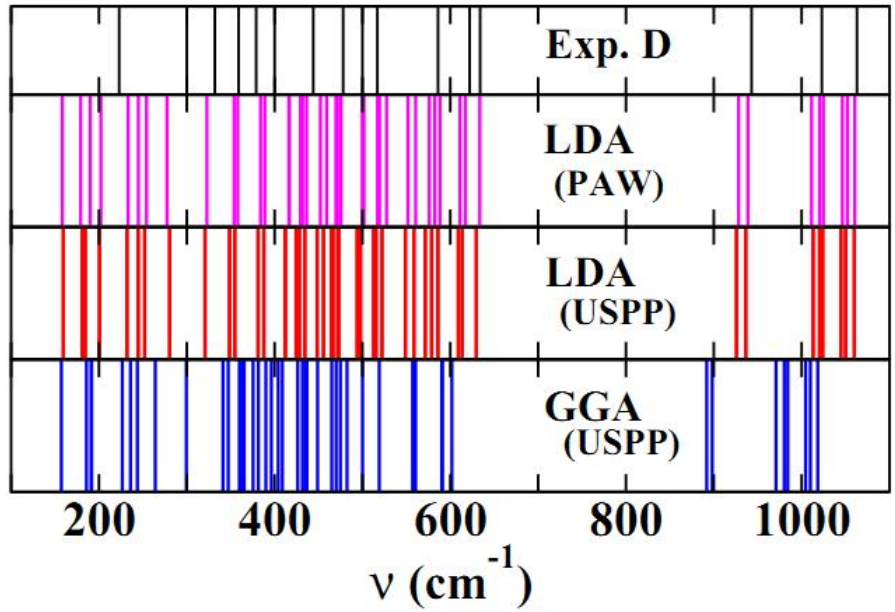

β-Li_3PO_4

A: B. N. Mavrin et al, J. Exp. Theor. Phys. **96**,53 (2003); B: F. Harbach and F. Fischer, Phys. Status Solidi B **66**, 237 (1974) – room temp. C: Ref. B at liquid nitrogen temp.; D: L. Popović et al, J. Raman Spectrosc. **34**,77 (2003).

Estimate of ionic conductivity assuming activated hopping

Schematic diagram of minimal energy path

Approximated using NEB algorithm[a]
– "Nudged Elastic Band"

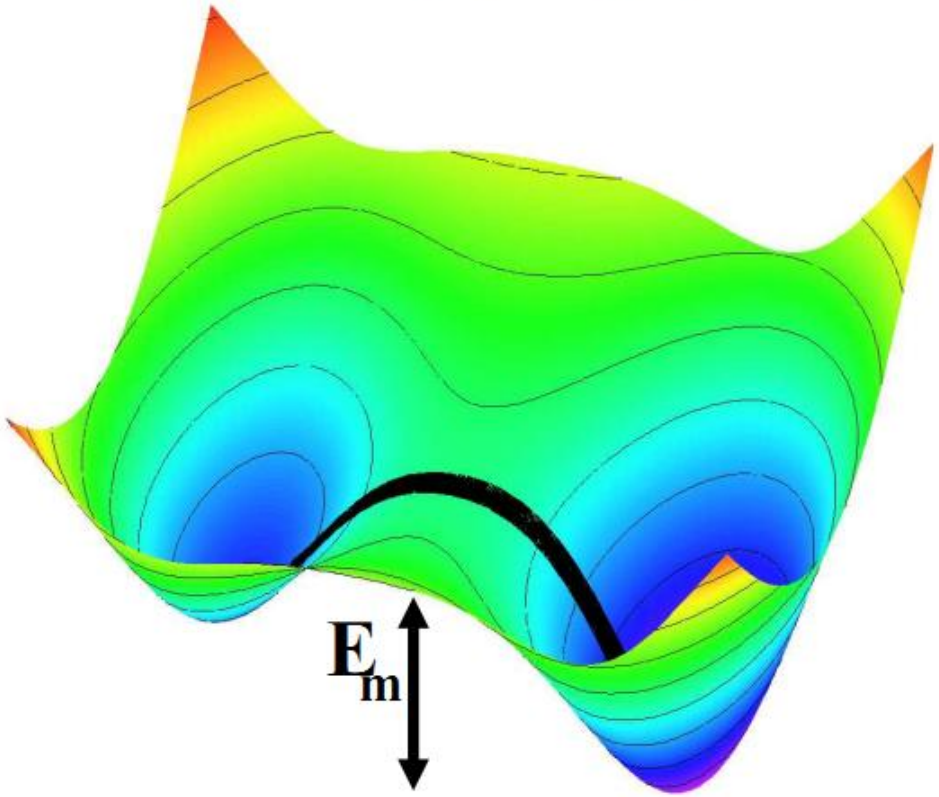

[a] Henkelman and Jónsson, *JCP* **113**, 9978 (2000)

Arrhenius relation

$$\sigma \cdot T = K\mathrm{e}^{-E_A/kT}$$

From: Ivanov-Shitz and co-workers, *Cryst. Reports* **46**, 864 (2001):

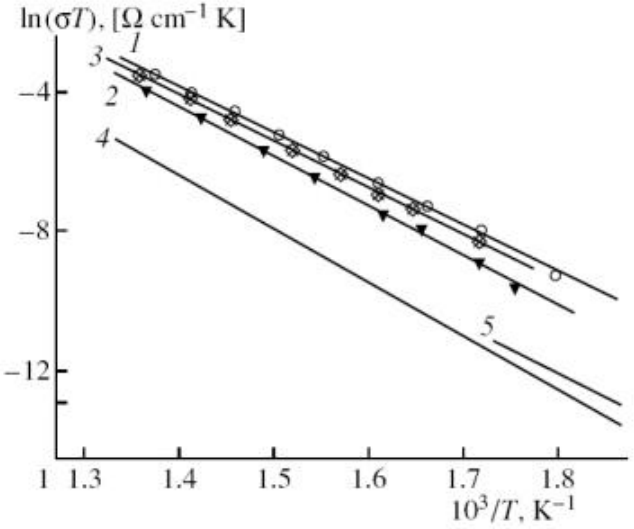

Fig. 2. Temperature dependences of conductivity in γ-Li_3PO_4: (*1*–*3*) for single crystals measured along the (*1*) *a*-axis, (*2*) *b*-axis, (*3*) *c*-axis and (*4*, *5*) for a polycrystal (*4*) according to [4, 5] and (*5*) according to [7].

E_A = 1.14, 1.23, 1.14, 1.31, 1.24 eV for 1,2,3,4,5, respectively.

➢ What is meant by “first principles”?

A series of well-controlled approximations

- ❑ Born-Oppenheimer Approximation
- ❑ Density Functional Approximation
- ❑ Local density Approximation (LDA)
- ❑ Numerical method: Projector Augmented Wave

Validation

- ❑ Lattice vibration modes
- ❑ Heats of formation
- ❑ Activation energies for lattice migration

WAKE FOREST UNIVERSITY

- **What is the interest in solid electrolytes?**

Materials components of a Li ion battery

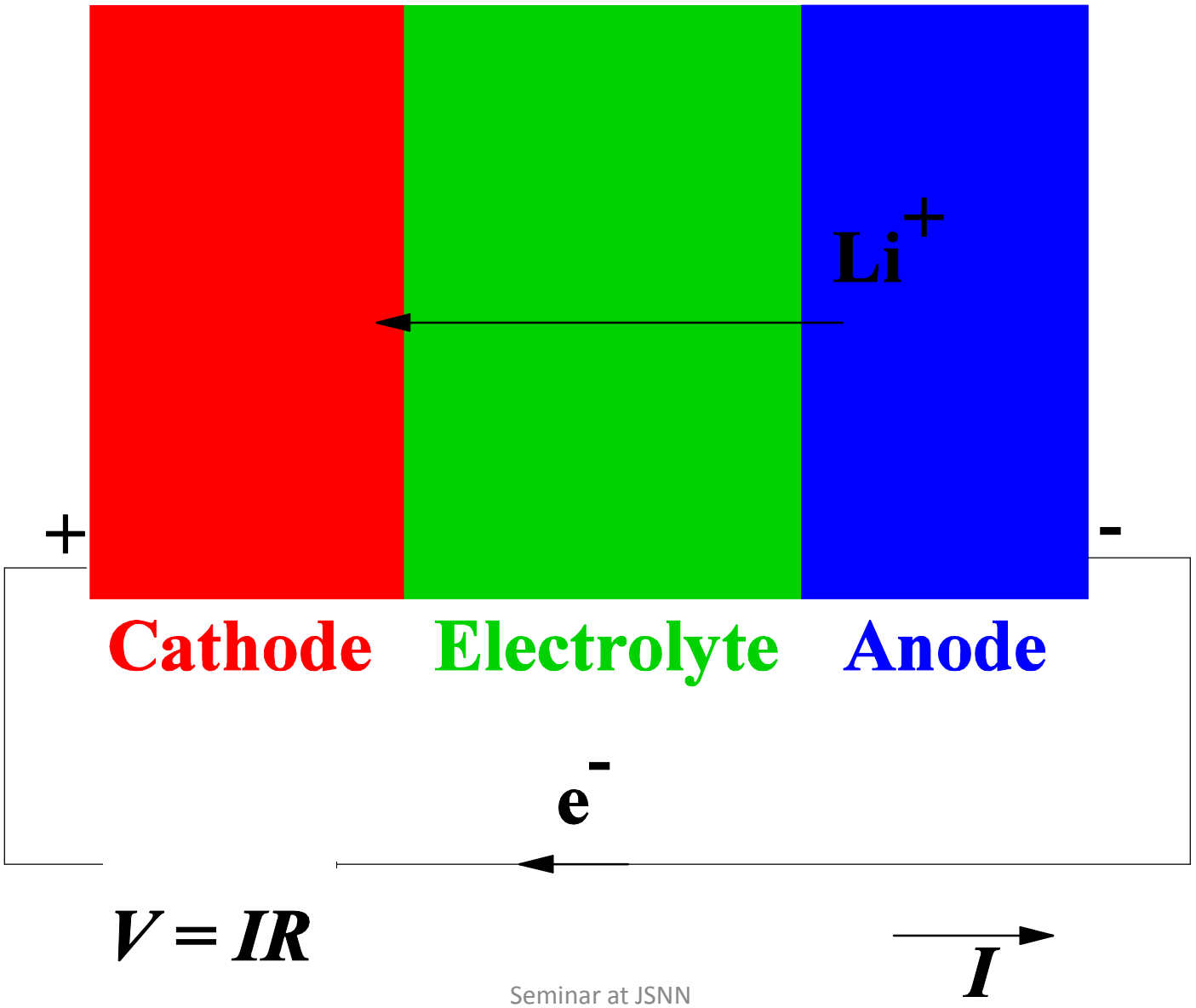

Example: Thin-film battery developed by Nancy Dudney and collaborators at Oak Ridge National Laboratory – **LiPON** (lithium phosphorus oxinitride)

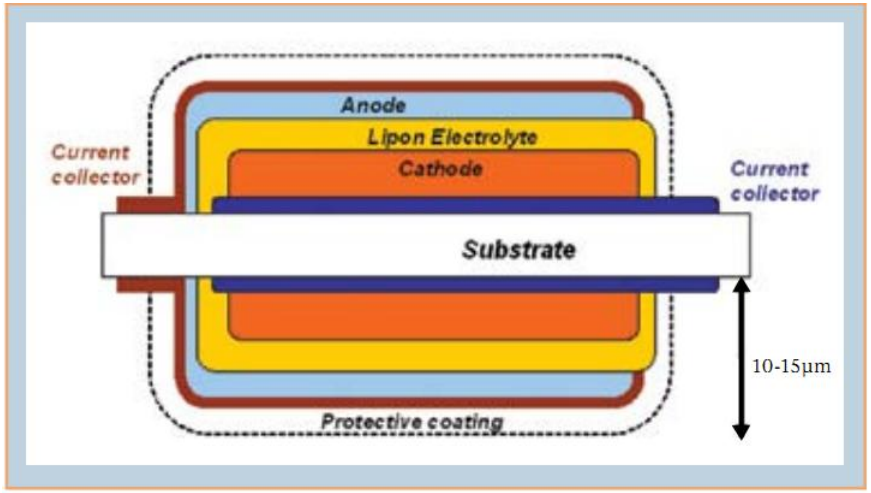

Fig. 1. *Schematic cross section of a thin film battery fabricated by vapor deposition onto both sides of a substrate support.*

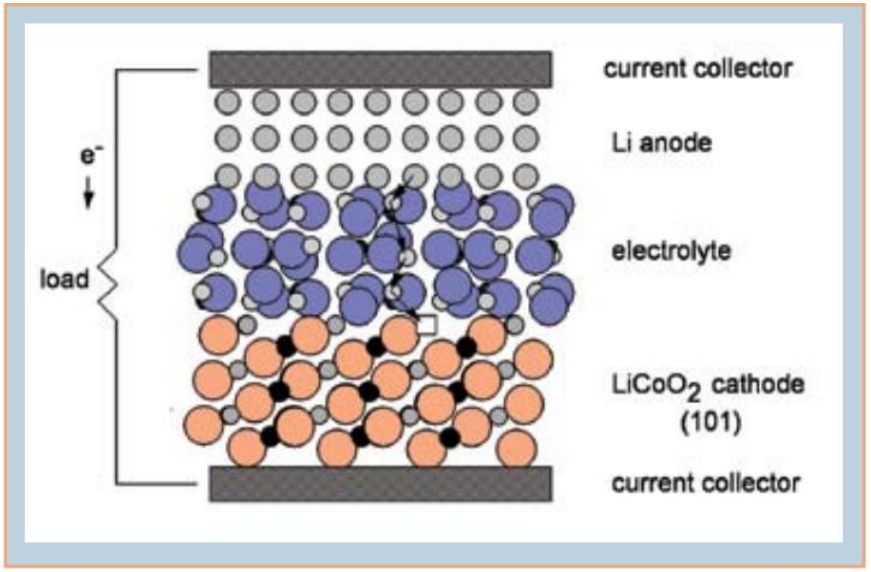

Fig. 2. *Schematic illustration of a thin film battery. The arrows indicate the discharge reaction where a Li ion diffuses from the lithium metal anode to fill a vacancy in an intercalation compound that serves as the cathode. The compensating electron is conducted through the device.*

From: N. J. Dudney, ***Interface* 77**(3) 44 (2008)

Solid *vs* liquid electrolytes in Li ion batteries

Solid electrolytes

Advantages

1. Excellent chemical and physical stability.
2. Perform well as thin film (≈1μ)
3. Li^+ conduction only (excludes electrons).

Disadvantages

1. Reduced contact area for high capacity electrodes.
2. Interface stress due to electrode charging and discharging.
3. Relatively low ionic conductivity.

Liquid electrolytes

Advantages

1. Excellent contact area with high capacity electrodes.
2. Can accommodate size changes of electrodes during charge and discharge cycles.
3. Relatively high ionic conductivity.

Disadvantages

1. Relatively poor physical and chemical stability.
2. Relies on the formation of "solid electrolyte interface" (SEI) layer.
3. May have both Li^+ and electron conduction.

From MRS Bulletin 39 1046-1049 Dec. 2014

Arthur Robinson and Jürgen Janek

"All-solid-state batteries are an emerging option for next-generation technologies"

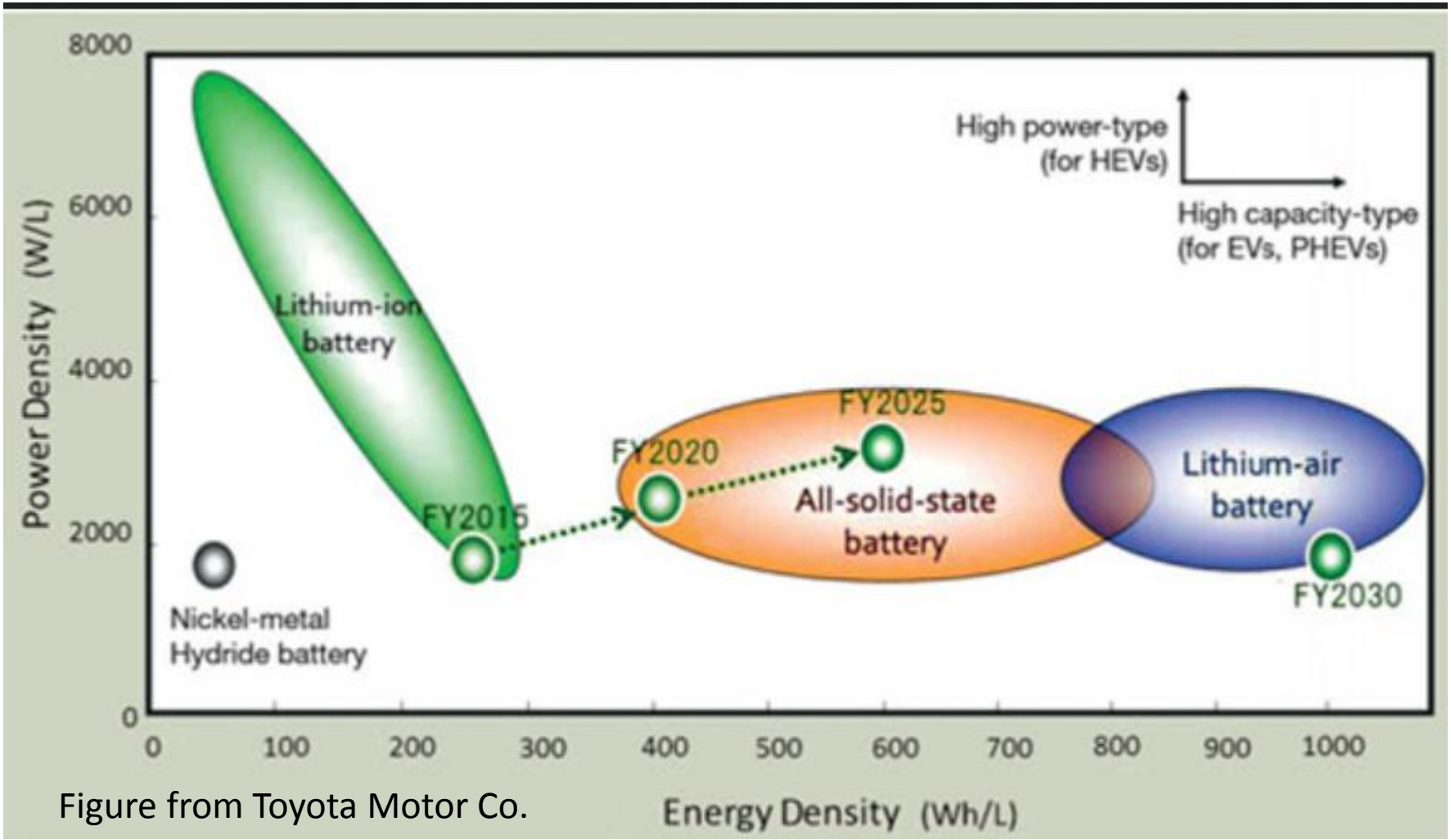

Figure from Toyota Motor Co.

Motivation: Paper by N. Kayama, *et. al* in ***Nature Materials*** **10**, 682-686 (2011)

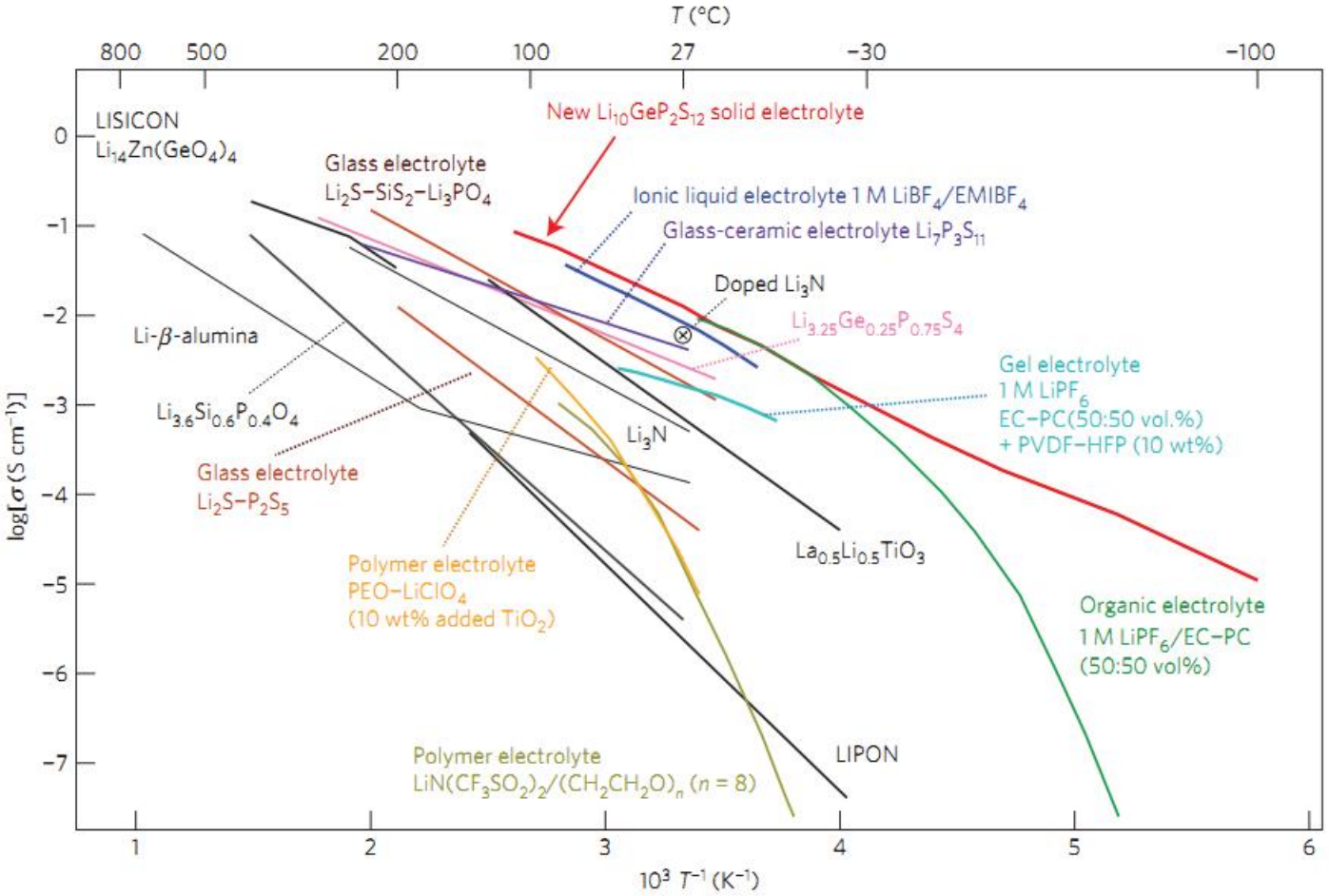

Figure 3 | Thermal evolution of ionic conductivity of the new $Li_{10}GeP_2S_{12}$ phase, together with those of other lithium solid electrolytes, organic liquid electrolytes, polymer electrolytes, ionic liquids and gel electrolytes[3-8,13-16,20,22]**.** The new $Li_{10}GeP_2S_{12}$ exhibits the highest lithium ionic conductivity (12 m S cm^{-1} at 27 °C) of the solid lithium conducting membranes of inorganic, polymer or composite systems. Because organic electrolytes usually have transport numbers below 0.5, inorganic lithium electrolytes have extremely high conductivities.

Motivation: Paper by N. Kamaya, *et. al* in ***Nature Materials*** **10**, 682-686 (2011)

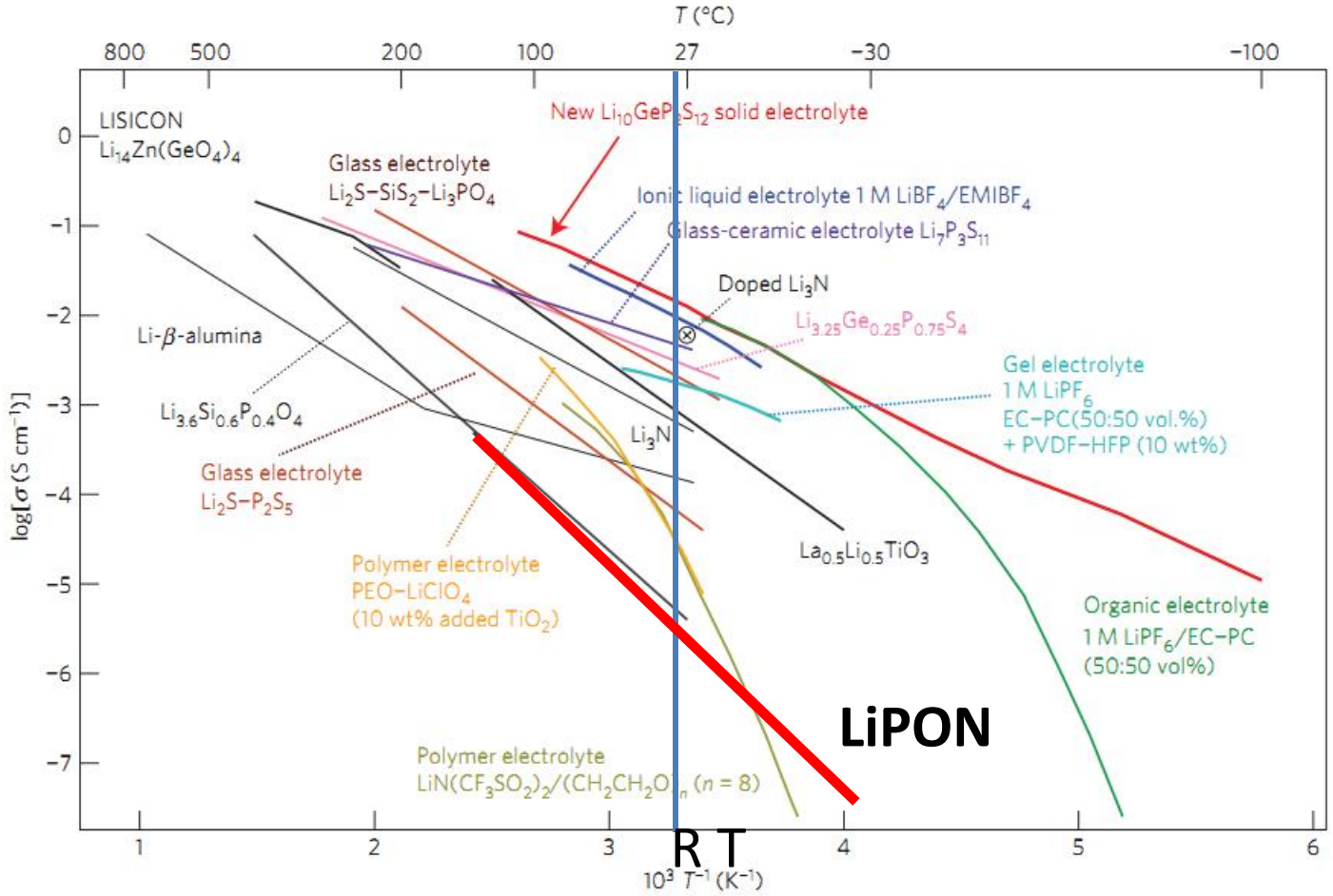

Figure 3 | Thermal evolution of ionic conductivity of the new $Li_{10}GeP_2S_{12}$ phase, together with those of other lithium solid electrolytes, organic liquid electrolytes, polymer electrolytes, ionic liquids and gel electrolytes[3-8,13-16,20,22]**.** The new $Li_{10}GeP_2S_{12}$ exhibits the highest lithium ionic conductivity (12 m S cm^{-1} at 27 °C) of the solid lithium conducting membranes of inorganic, polymer or composite systems. Because organic electrolytes usually have transport numbers below 0.5, inorganic lithium electrolytes have extremely high conductivities.

Motivation: Paper by N. Kamaya, *et. al* in ***Nature Materials*** **10**, 682-686 (2011)

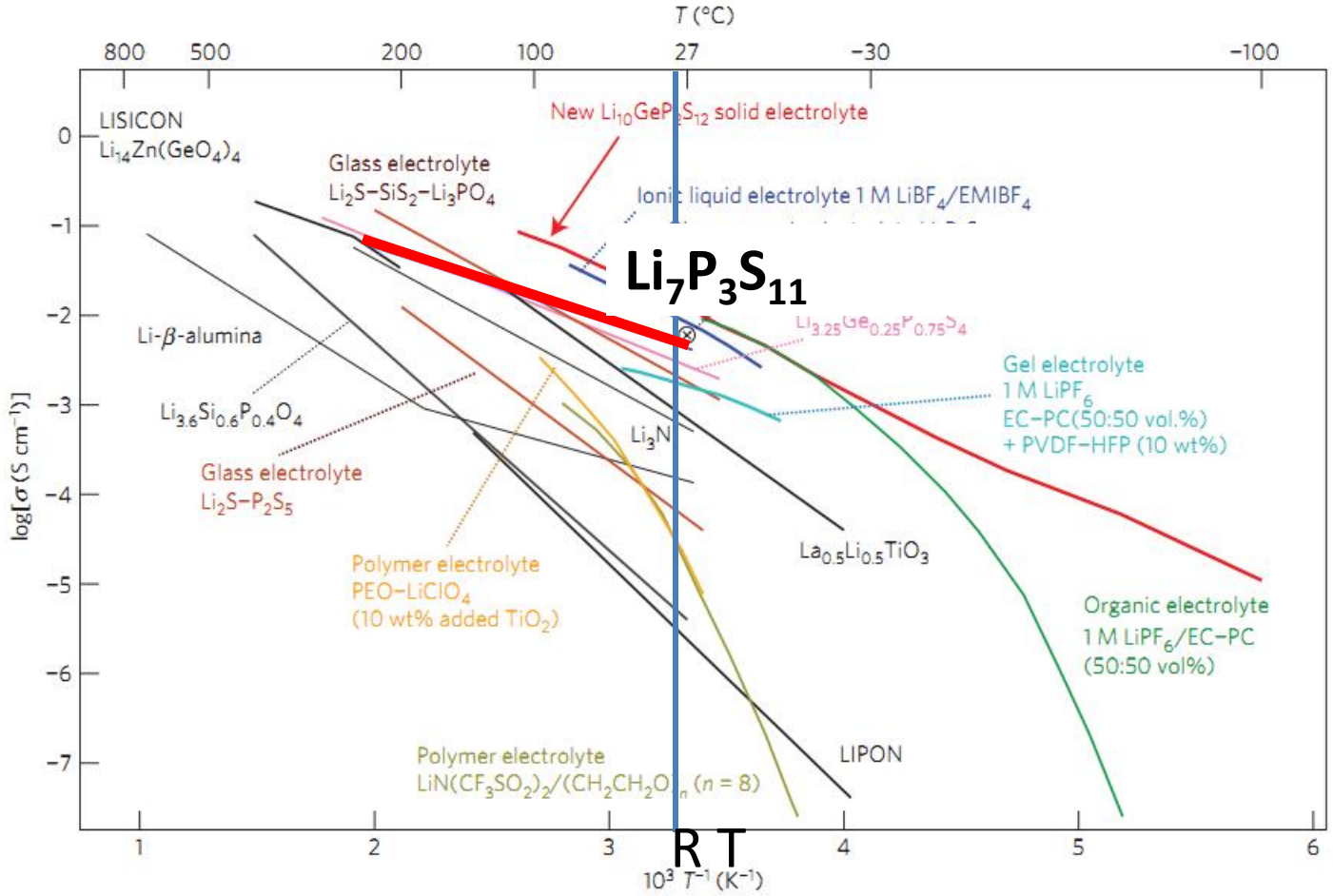

Figure 3 | Thermal evolution of ionic conductivity of the new $Li_{10}GeP_2S_{12}$ phase, together with those of other lithium solid electrolytes, organic liquid electrolytes, polymer electrolytes, ionic liquids and gel electrolytes[3-8,13-16,20,22]**.** The new $Li_{10}GeP_2S_{12}$ exhibits the highest lithium ionic conductivity (12 m S cm^{-1} at 27 °C) of the solid lithium conducting membranes of inorganic, polymer or composite systems. Because organic electrolytes usually have transport numbers below 0.5, inorganic lithium electrolytes have extremely high conductivities.

Motivation: Paper by N. Kamaya, *et. al* in ***Nature Materials*** **10**, 682-686 (2011)

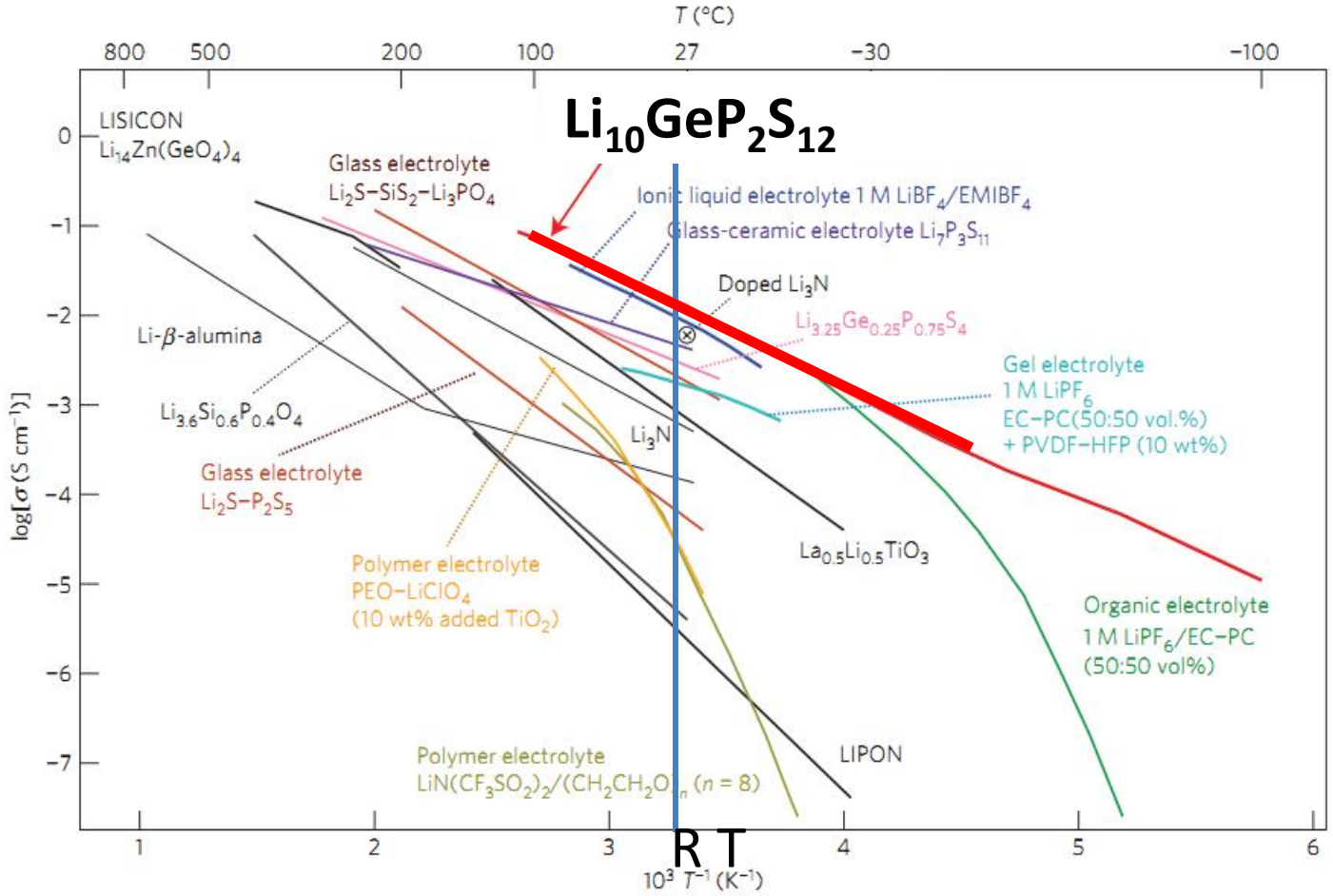

Figure 3 | Thermal evolution of ionic conductivity of the new $Li_{10}GeP_2S_{12}$ phase, together with those of other lithium solid electrolytes, organic liquid electrolytes, polymer electrolytes, ionic liquids and gel electrolytes[3-8,13-16,20,22]**.** The new $Li_{10}GeP_2S_{12}$ exhibits the highest lithium ionic conductivity (12 m S cm^{-1} at 27 °C) of the solid lithium conducting membranes of inorganic, polymer or composite systems. Because organic electrolytes usually have transport numbers below 0.5, inorganic lithium electrolytes have extremely high conductivities.

How can computer simulations contribute to the development of materials?

- Computationally examine known materials and predict new materials and their properties
  - Structural forms
  - Relative stabilities
  - Direct comparisons of simulations and experiment
  - Investigate properties that are difficult to realize experimentally

Of particular interest in battery materials --

- Model ion migration mechanisms
  - Vacancy migration
  - Interstitial migration
  - Vacancy-interstitial formation energies

The Li_2PO_2N story

Systematic study of LiPON materials – $Li_xPO_yN_z$ – (Yaojun A. Du and N. A. W. Holzwarth, Phys. Rev. B 81, 184106 (2010))

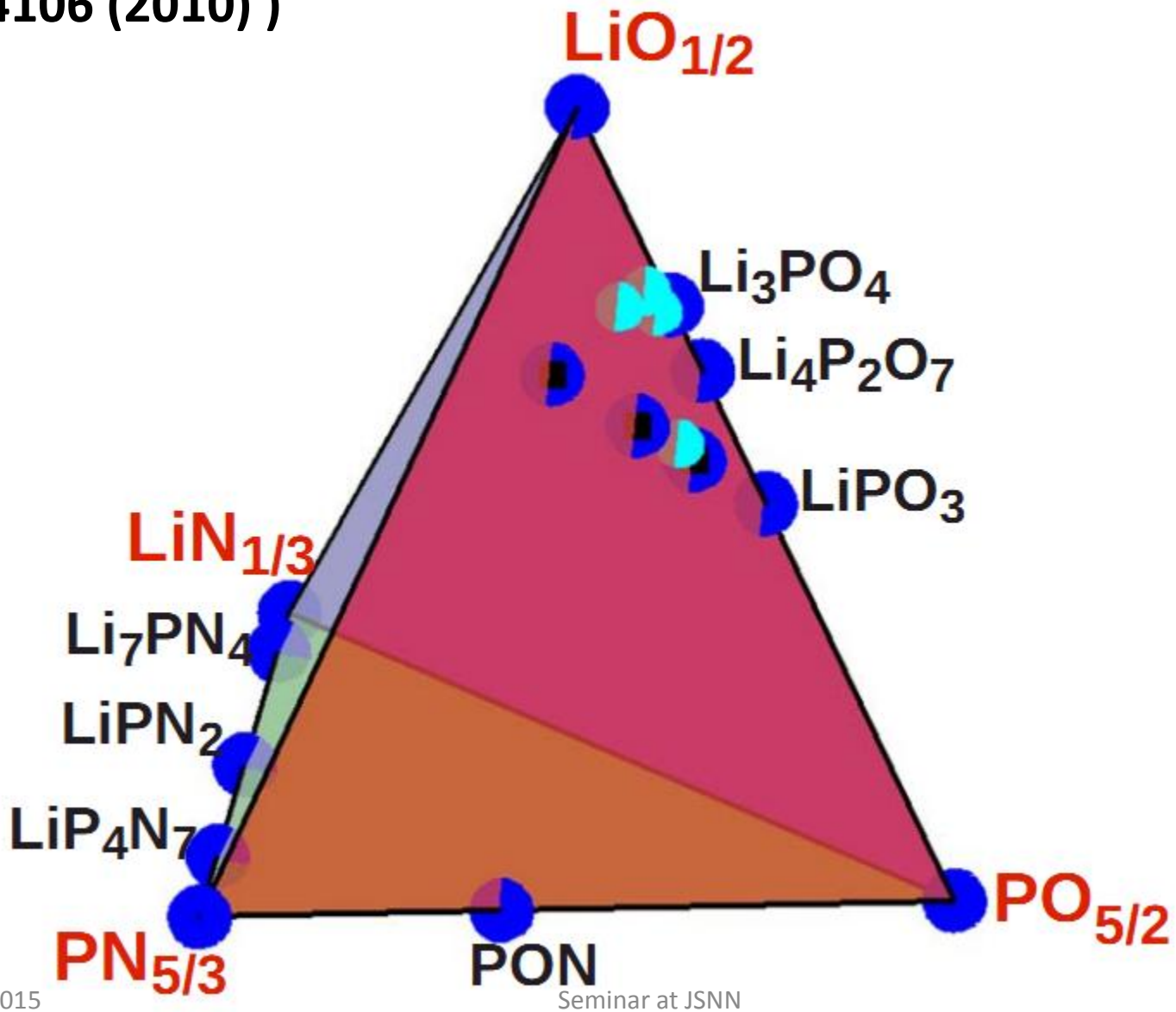

Table 1. Calculated heats of formation for Li phosphates, phospho-nitrides, and thiophosphates and related materials. The structural designation uses the the notation defined in the International Table of Crystallography[85] based on structural information reported in the International Crystal Structure Database.[86] The heats of formation ΔH (eV/FU) are given in units of eV per formula unit. When available from Ref. [31] and [32] experiment values are indicated in parentheses. Those indicated with "*" were used fitting the O and N reference energies as explained in the text.

Material	Structure	ΔH (eV/FU)
β-Li_3PO_4	$Pmn2_1$ (#31)	-21.23
γ-Li_3PO_4	$Pnma$ (#62)	-21.20 (-21.72*)
γ-Li_3PS_4	$Pmn2_1$ (#31)	- 8.37
β-Li_3PS_4	$Pnma$ (#62)	- 8.28
$Li_4P_2O_6$	$P\bar{3}1m$ (#162)	-29.72
$Li_4P_2O_7$	$P\bar{1}$ (#2)	-33.97
$Li_5P_2O_6N$	$P\bar{1}$ (#2)	-33.18
$Li_4P_2S_6$	$P\bar{3}1m$ (#162)	-12.42
$Li_4P_2S_7$	$P\bar{1}$ (#2)	-11.59
$Li_7P_3O_{11}$	$P\bar{1}$ (#2)	-54.84
$Li_7P_3S_{11}$	$P\bar{1}$ (#2)	-20.01
$LiPO_3$	$P2/c$ (#13)	-12.75
$LiPN_2$	$I\bar{4}2d$ (#122)	- 3.65
$s1$-Li_2PO_2N	$Pbcm$ (#57)	-12.35
SD-Li_2PO_2N	$Cmc2_1$ (#36)	-12.47
SD-Li_2PS_2N	$Cmc2_1$ (#36)	- 5.80

Material	Structure	ΔH (eV/FU)
N_2O_5	$P6_3/mmc$ (#194)	- 0.94 (- 0.45*)
P_3N_5	$C2/c$ (#15)	- 3.02 (- 3.32*)
h-P_2O_5	$R3c$ (#161)	-15.45 (-15.53*)
o-P_2O_5	$Fdd2$ (#43)	-15.78
P_2S_5	$P\bar{1}$ (#2)	- 1.93
P_4S_3	$Pnma$ (#62)	- 2.45 (- 2.33)
SO_3	$Pna2_1$ (#33)	- 4.84 (- 4.71*)
Li_3N	$P6/mmm$ (#191)	- 1.60 (- 1.71*)
Li_2O	$Fm\bar{3}m$ (#225)	- 6.10 (- 6.20*)
Li_2O_2	$P6_3/mmc$ (#194)	- 6.35 (- 6.57*)
Li_3P	$P6_3/mmc$ (#194)	- 3.47
Li_2S	$Fm\bar{3}m$ (#225)	- 4.30 (- 4.57)
Li_2S_2	$P6_3/mmc$ (#194)	- 4.09
$LiNO_3$	$R\bar{3}c$ (#167)	- 5.37 (- 5.01*)
Li_2SO_4	$P2_1/c$ (#14)	-14.63 (-14.89*)

Phosphate chain materials: $LiPO_3$ plus N

$LiPO_3$ in $P2/c$ structure; 100 atom unit cell

Chain direction perpendicular to plane of diagram

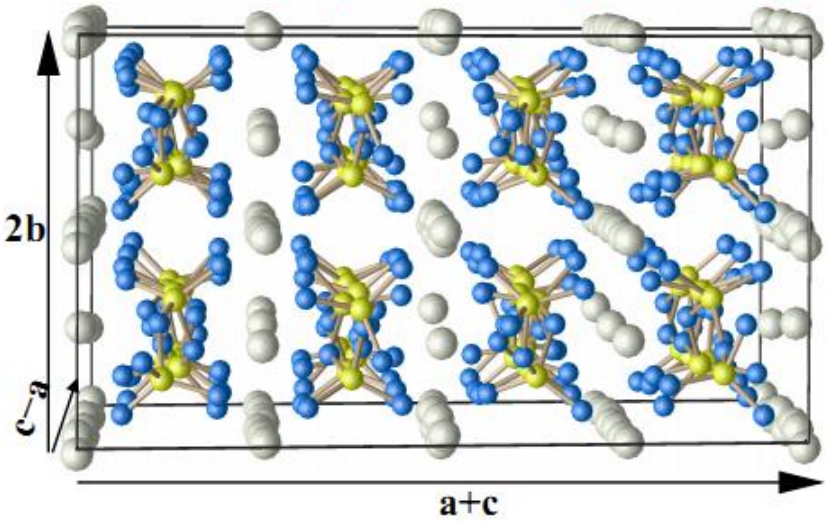

Ball colors: =Li, =P, =O.

Single chain view

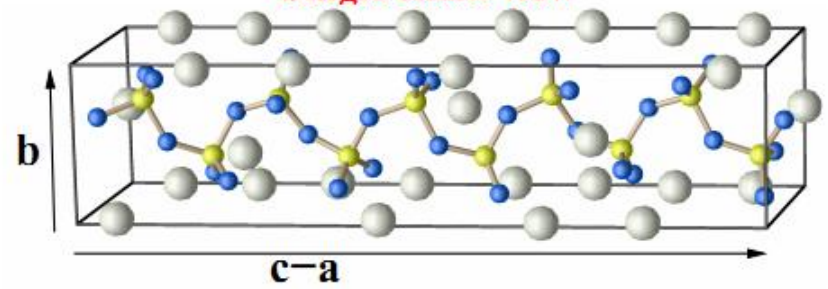

s_1-Li_2PO_2N in $Pbcm$ structure; 24 atom unit cell

Chain direction perpendicular to plane of diagram

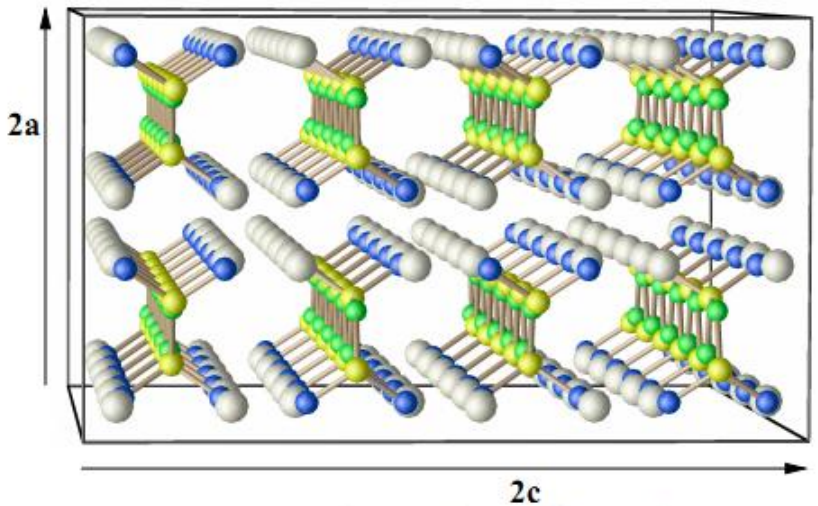

Ball colors: =Li, =P, =O, =N.

Single chain view

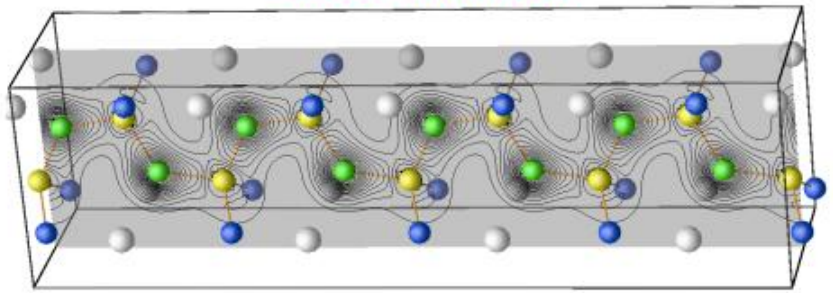

Two forms of Li_2PO_2N

Li ion

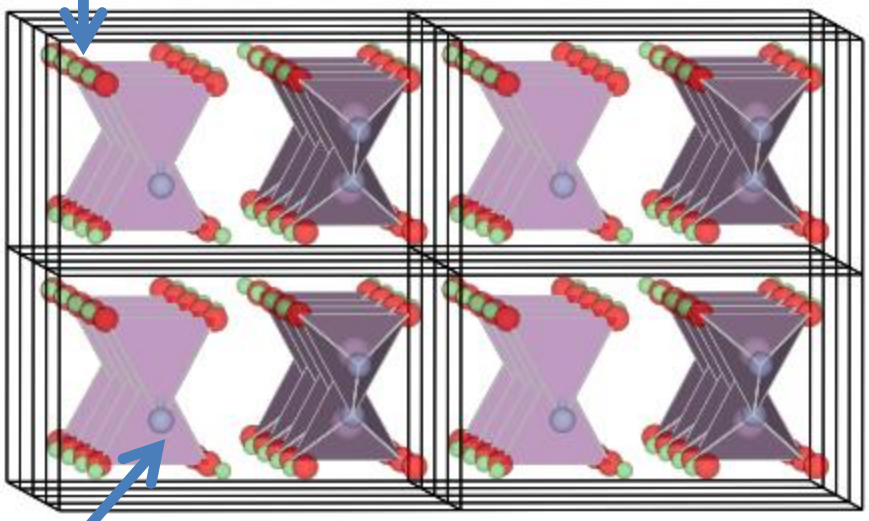

PO_2N_2 ion

s_1-Li_2PO_2N *(Pbcm)*

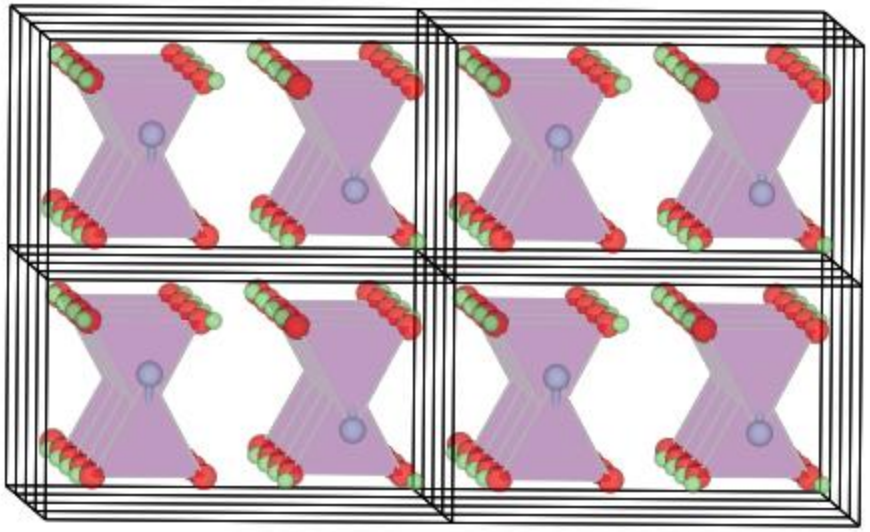

s_2-Li_2PO_2N *(Aem2)*

Possible exothermic reaction pathways:

$$\tfrac{1}{5}P_2O_5 + \tfrac{1}{5}P_3N_5 + Li_2O \rightarrow Li_2PO_2N + 2.5\,\text{eV}.$$

$$Li_2O_2 + \tfrac{1}{5}P_3N_5 + \tfrac{2}{5}P \rightarrow Li_2PO_2N + 5.3\,\text{eV}.$$

$$LiNO_3 + Li + P \rightarrow Li_2PO_2N + \tfrac{1}{2}O_2 + 7.0\,\text{eV}.$$

Synthesis of Li_2PO_2N by Keerthi Senevirathne, Cynthia Day, Michael Gross, and Abdessadek Lachgar

Method: High temperature solid state synthesis based on reaction

$$Li_2O + \tfrac{1}{5}P_2O_5 + \tfrac{1}{5}P_3N_5 \rightarrow Li_2PO_2N$$

Structure from X-ray refinement: $Cmc2_1$

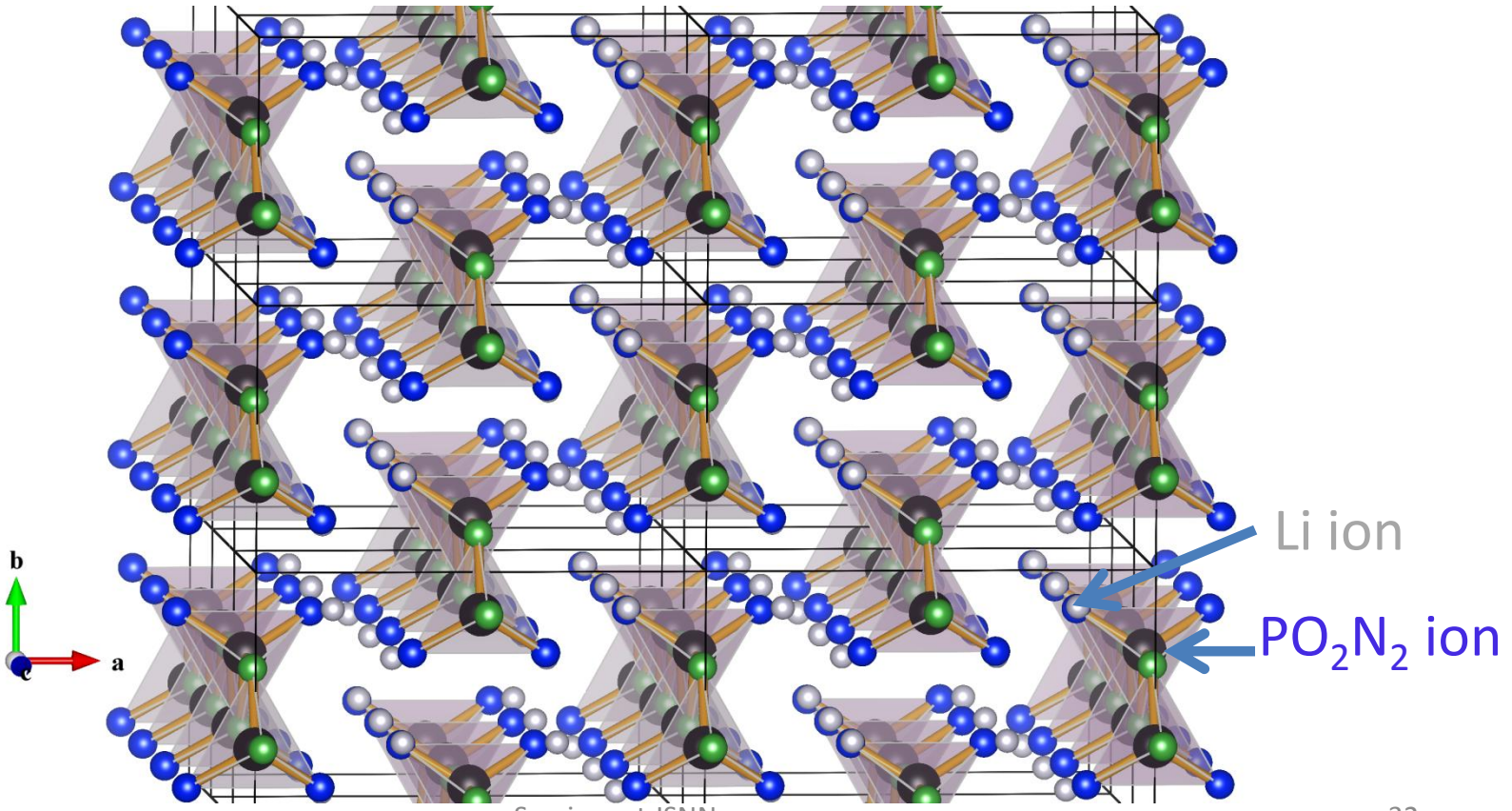

Comparison of synthesized and predicted structures of Li_2PO_2N:

WAKE FOREST UNIVERSITY

Synthesized

Predicted

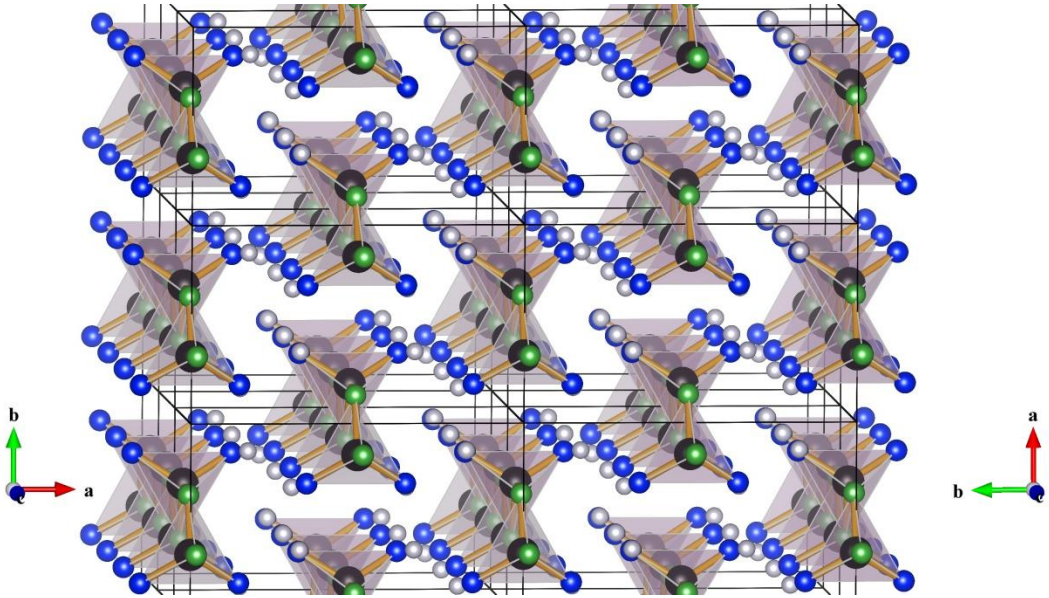

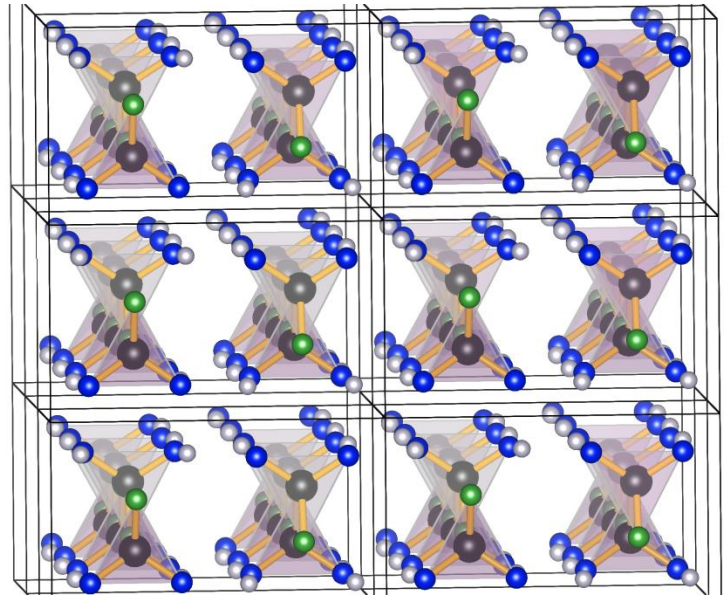

Li P O N

***SD*-Li_2PO_2N (*$Cmc2_1$*)**

***s_2*-Li_2PO_2N (*Aem2*)**

Calculations have now verified that the SD structure is more stable than the s_2 structure by 0.1 eV/FU.

WAKE FOREST UNIVERSITY

Comparison of synthesized Li_2PO_2N with Li_2SiO_3

SD-Li_2PO_2N (*Cmc2₁*)

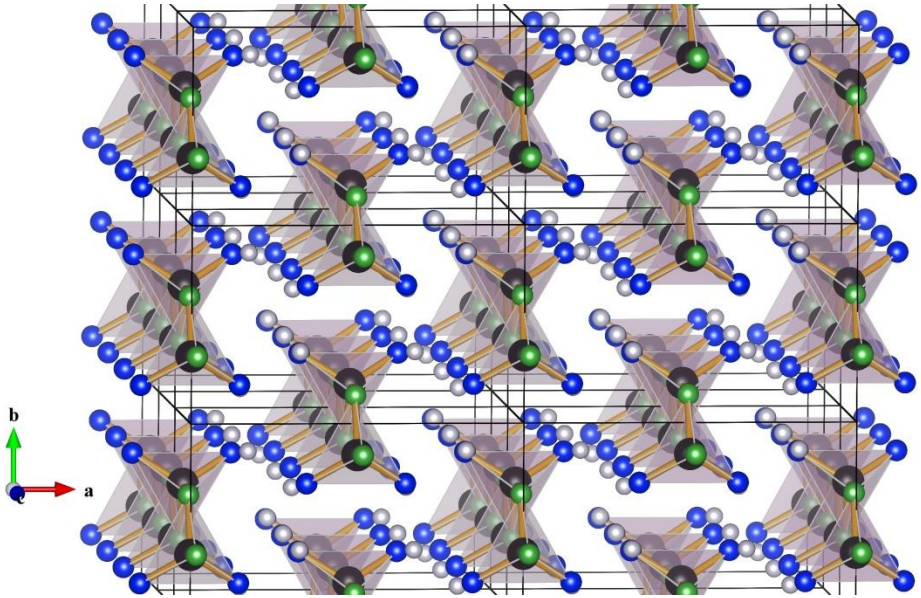

a=9.07 Å, b=5.40 Å, c=4.60 Å

Li_2SiO_3 (*Cmc2₁*)

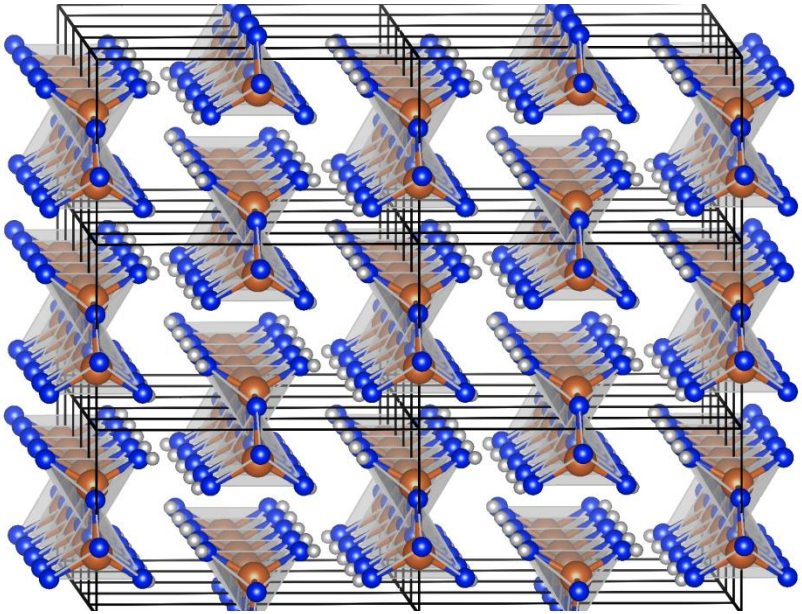

a=9.39 Å, b=5.40 Å, c=4.66 Å

K.-F. Hesse, Acta Cryst. B33, 901 (1977)

Li P O N Si

Electronic band structure of *SD*-Li_2PO_2N

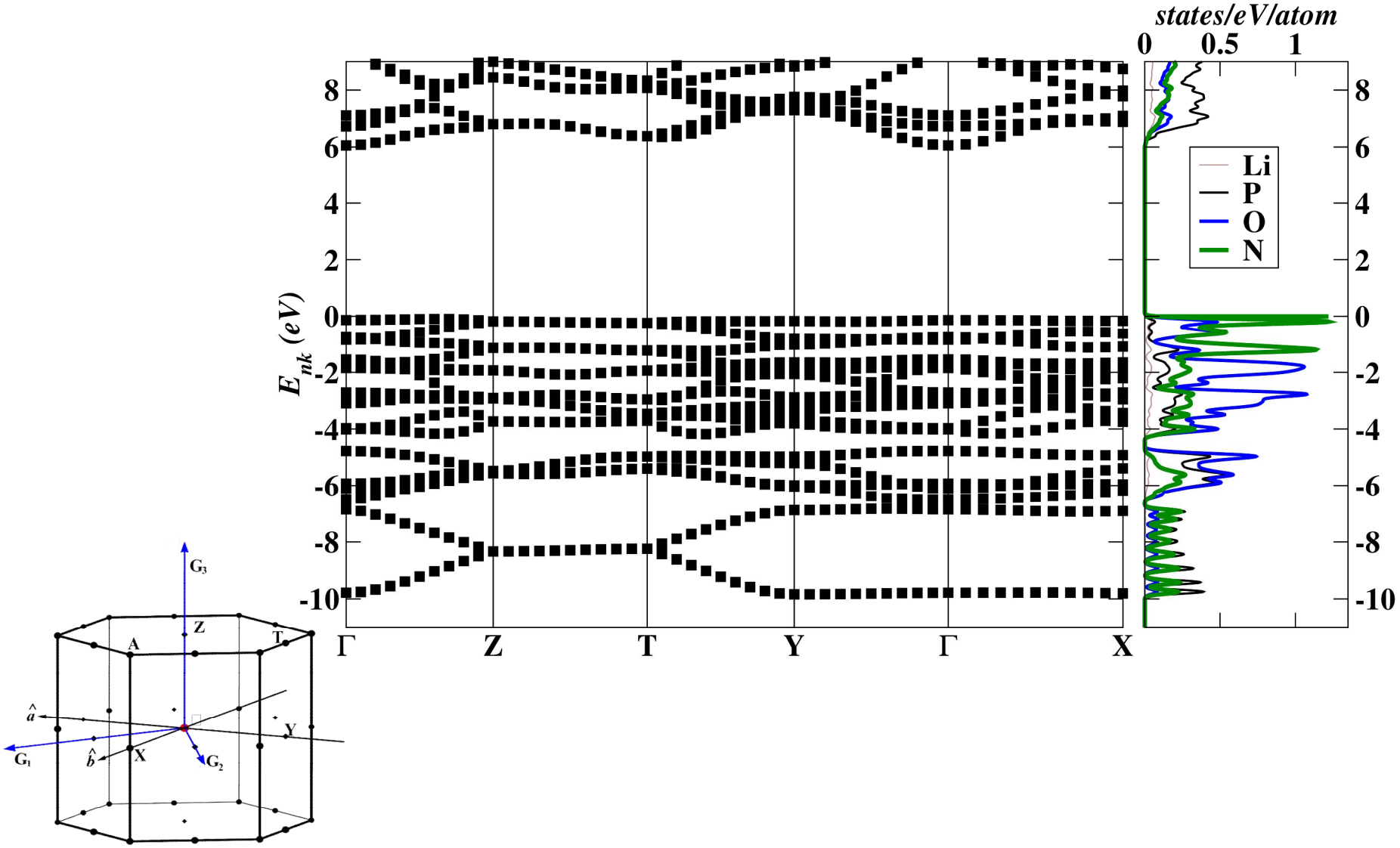

More details of *SD*-Li_2PO_2N structure

Ball and stick model

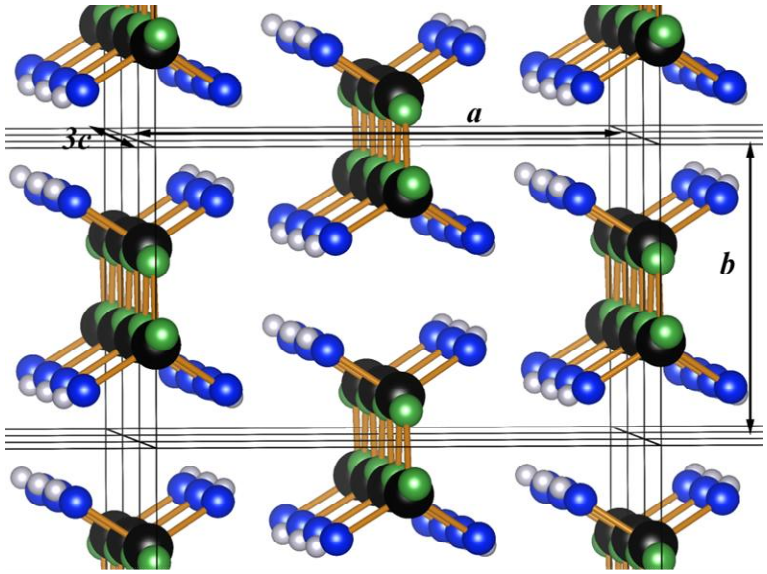

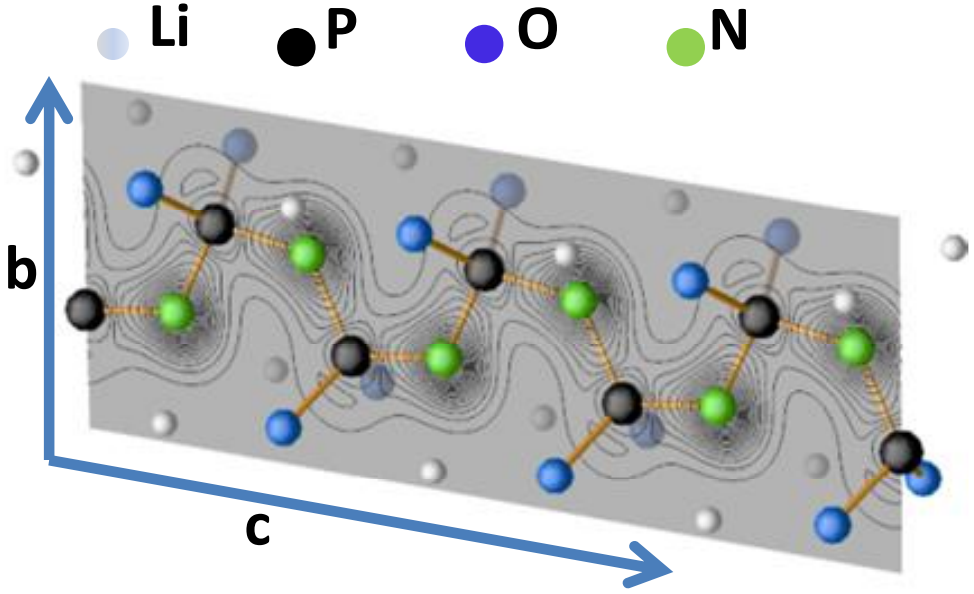

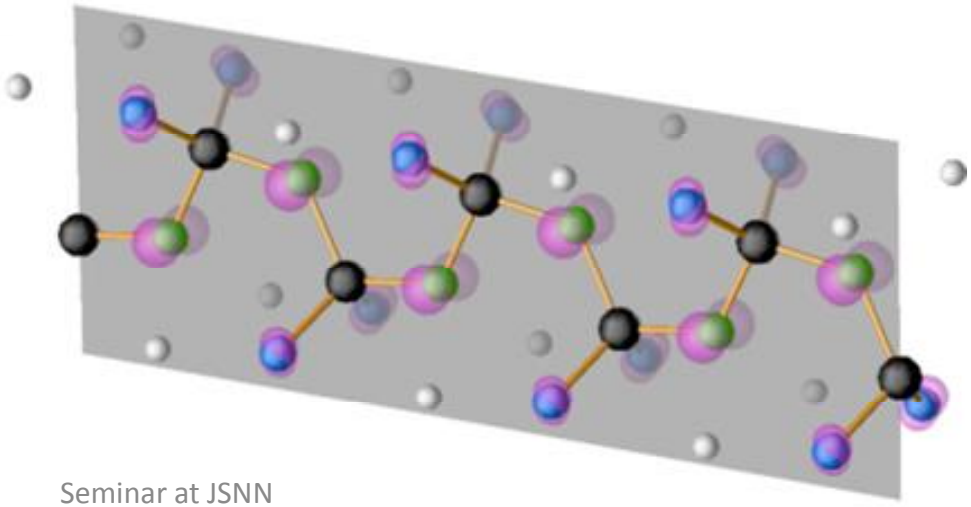

Isosurfaces (maroon) of charge density of states at top of valence band, primarily π states on N.

Vibrational spectrum of *SD*-Li_2PO_2N

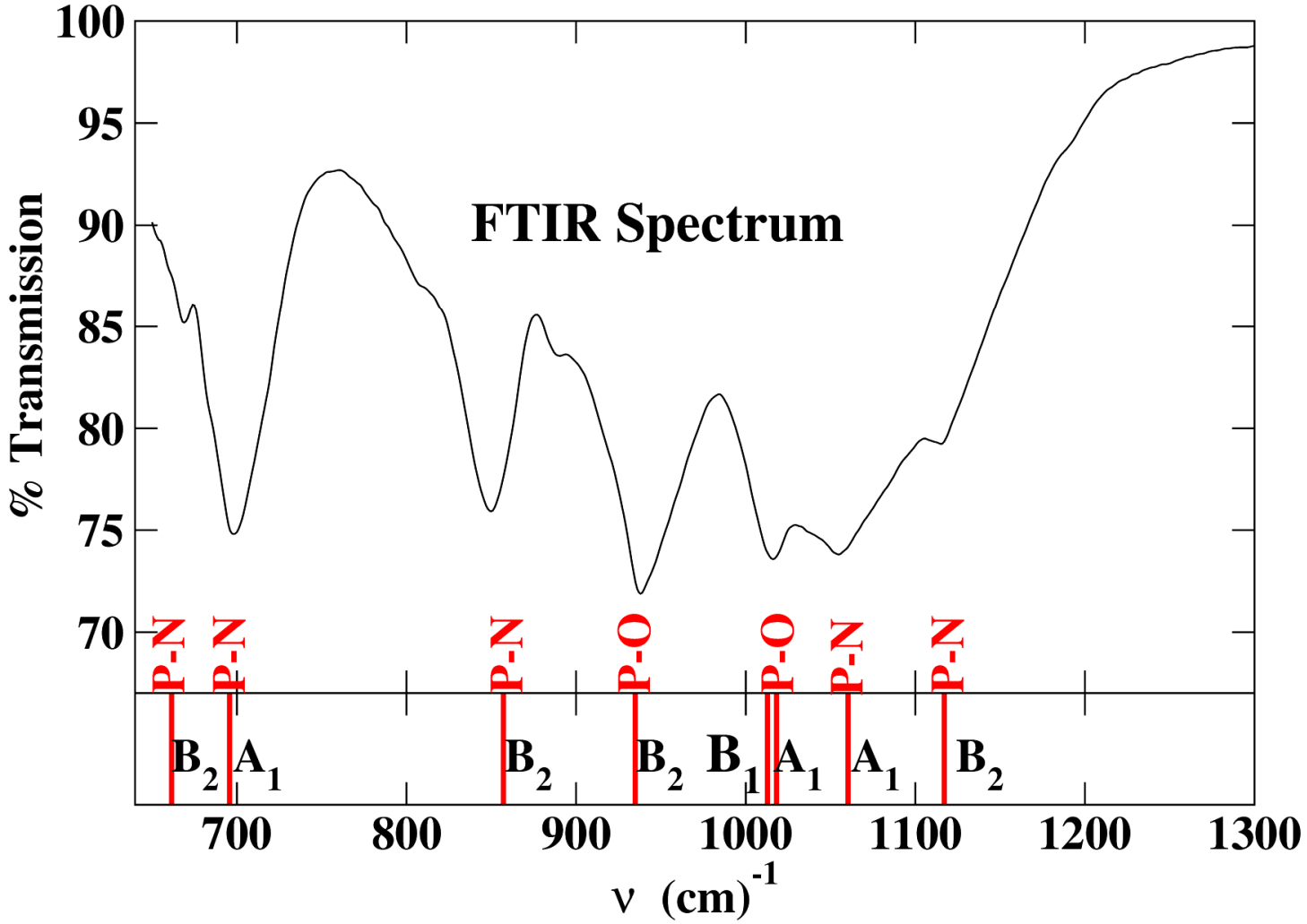

Stability of *SD*-Li_2PO_2N in air

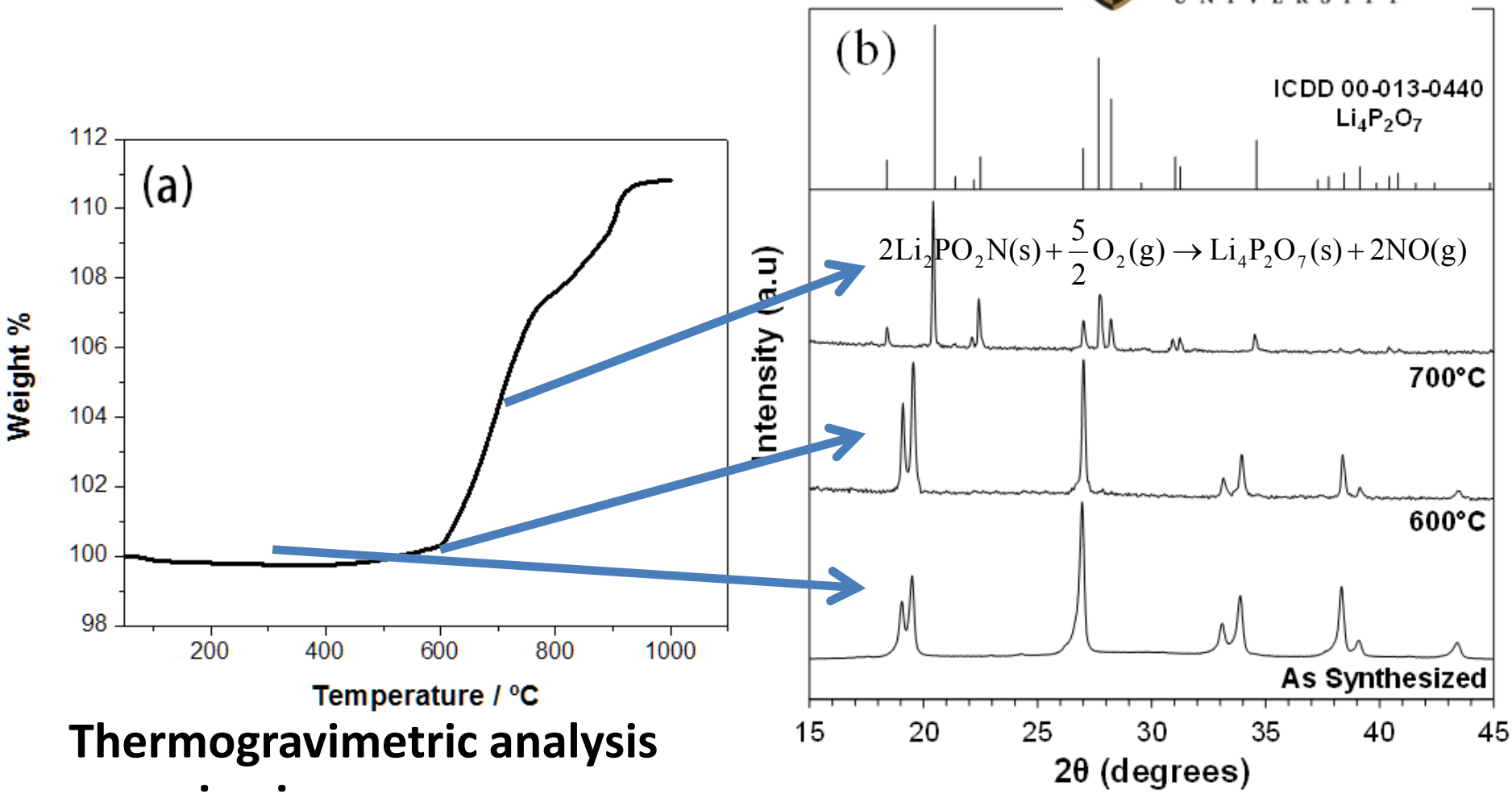

Thermogravimetric analysis curve in air

Note: no structural changes were observed while heating in vacuum up to 1050° C.

Ionic conductivity of *SD*-Li_2PO_2N

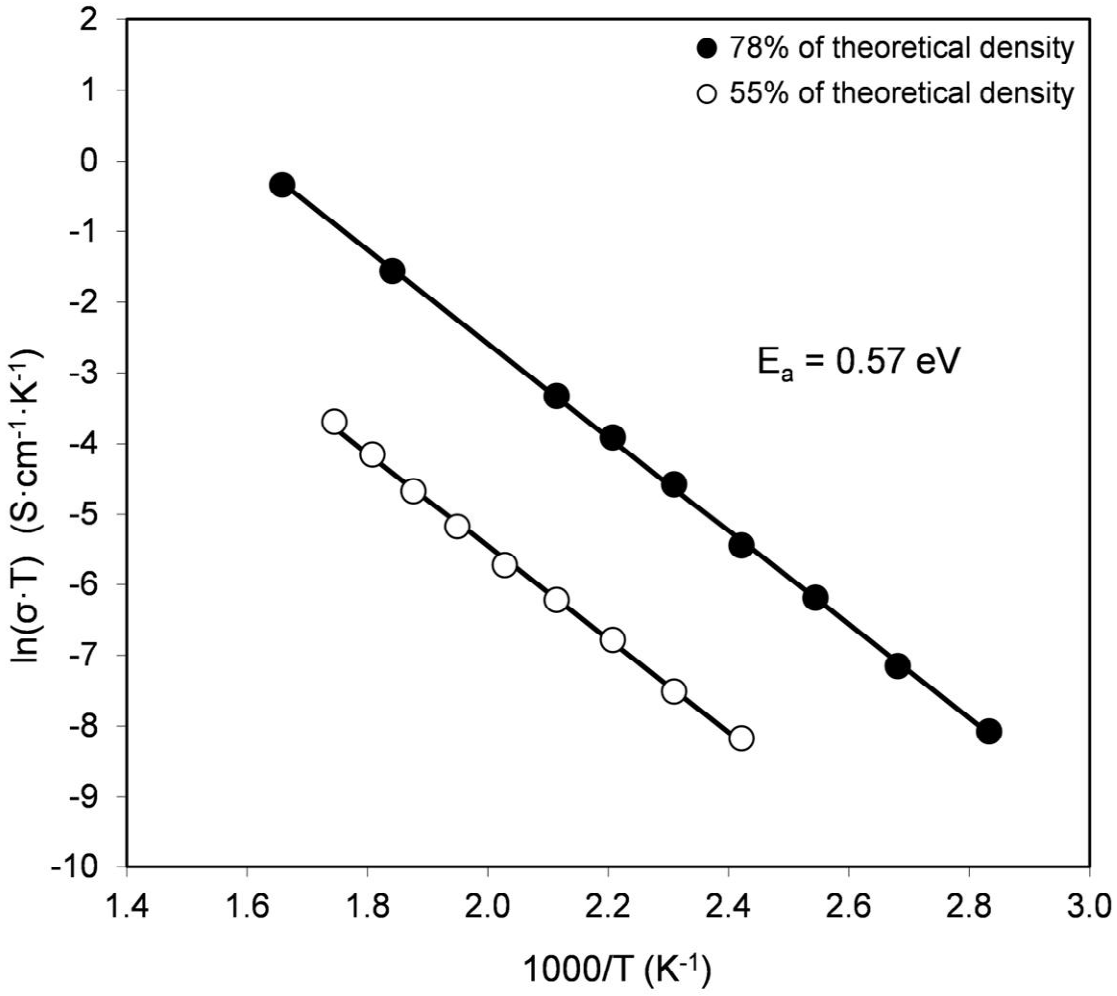

NEB analysis of E_m (vacancy mechanism)

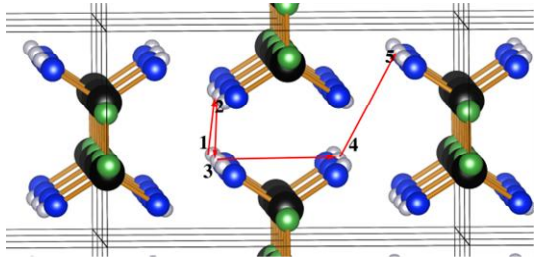

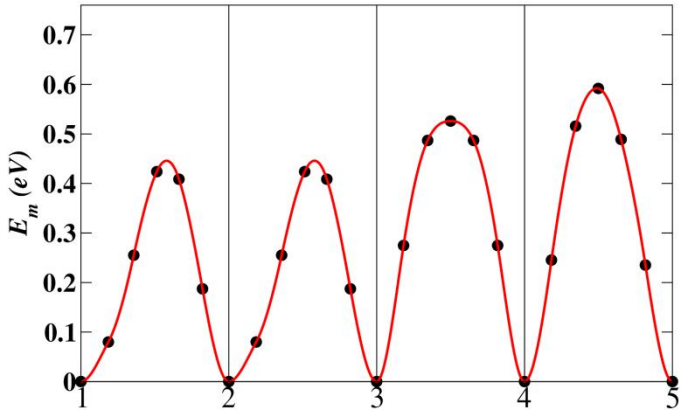

Summary of measured and calculated conductivity parameters in $Li_xPO_yN_z$ materials

Measured activation energies E_A^{exp} compared with calculated migration energies for vacancy (E_m^{cal} (vac.)) and interstitial (E_m^{cal} (int.)) mechanisms and vacancy-interstitial formation energies (E_f^{cal}). All energies are given in eV.

Material	Form	E_A^{exp}	E_m^{cal} (vac.)	E_m^{cal} (int.)	E_f^{cal}	E_A^{cal}
γ-Li_3PO_4	single crystal[a]	1.23, 1.14	0.7, 0.7	0.4, 0.3	1.7	1.3, 1.1
$Li_{2.88}PO_{3.73}N_{0.14}$	poly cryst.	0.97				
$Li_{3.3}PO_{3.9}N_{0.17}$	amorphous	0.56				
$Li_{1.35}PO_{2.99}N_{0.13}$	amorphous	0.60				
$LiPO_3$	poly cryst.	1.4	0.6, 0.7	0.7	1.2	1.1-1.2
$LiPO_3$	amorphous	0.76-1.2				
s_1-Li_2PO_2N	single crystal		0.5, 0.6		1.7	1.3-1.5
$LiPN_2$	poly cryst.	0.6	0.4		2.5	1.7
Li_7PN_4	poly cryst.	0.5				

Summary of the Li_2PO_2N story

- Predicted on the basis of first principles theory
- Subsequently, experimentally realized by Keerthi Seneviranthe and colleagues; generally good agreement between experiment and theory
- Ion conductivity properties not (yet) competitive

Simulations of other solid electrolytes and electrolyte/electrode interfaces

From ORNL: Experiment on electrolyte Li_3PS_4

WAKE FOREST UNIVERSITY

JACS
JOURNAL OF THE AMERICAN CHEMICAL SOCIETY
Communication
pubs.acs.org/JACS

Anomalous High Ionic Conductivity of Nanoporous β-Li_3PS_4

Zengcai Liu,[†] Wujun Fu,[†] E. Andrew Payzant,[†,‡] Xiang Yu,[†] Zili Wu,[†,§] Nancy J. Dudney,[‡] Jim Kiggans,[‡] Kunlun Hong,[†] Adam J. Rondinone,[†] and Chengdu Liang*,[†]

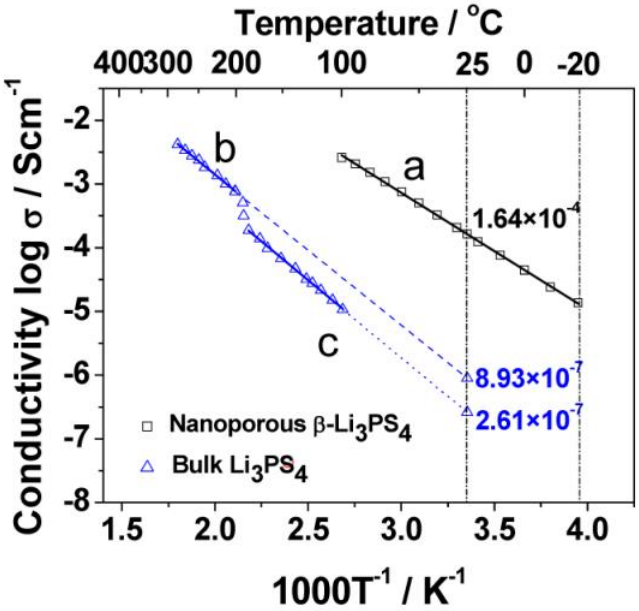

Figure 1. Arrhenius plots for nanoporous β-Li_3PS_4 (line a), bulk β-Li_3PS_4 (line b), and bulk γ-Li_3PS_4 (line c). The conductivity data for bulk Li_3PS_4 are reproduced from the work of Tachez.[10].

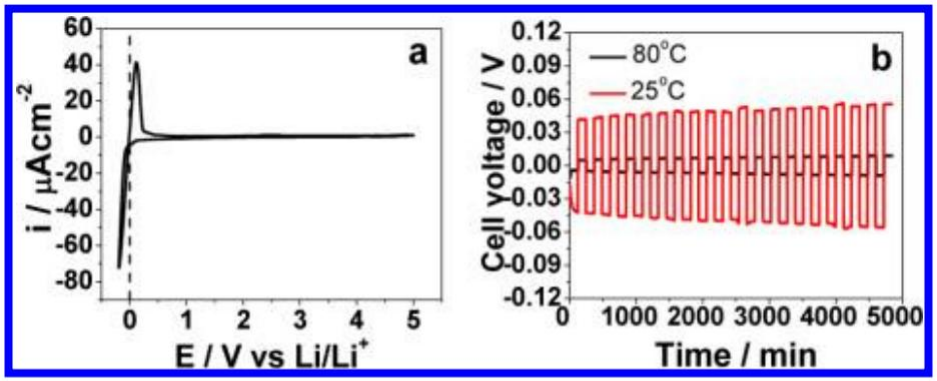

Figure 5. Electrochemical stability of β-Li_3PS_4 and cycling stability with metallic lithium electrodes. (a) CV of a Li/β-Li_3PS_4/Pt cell, where Li and Pt serve as the reference/counter and working electrodes, respectively. (b) Lithium cyclability in a symmetric Li/β-Li_3PS_4/Li cell. The cell was cycled at a current density of 0.1 mA cm^{-2} at room temperature and 80 °C.

Crystal structure of bulk Li_3PS_4 – γ-form $Pmn2_1$ (#31)

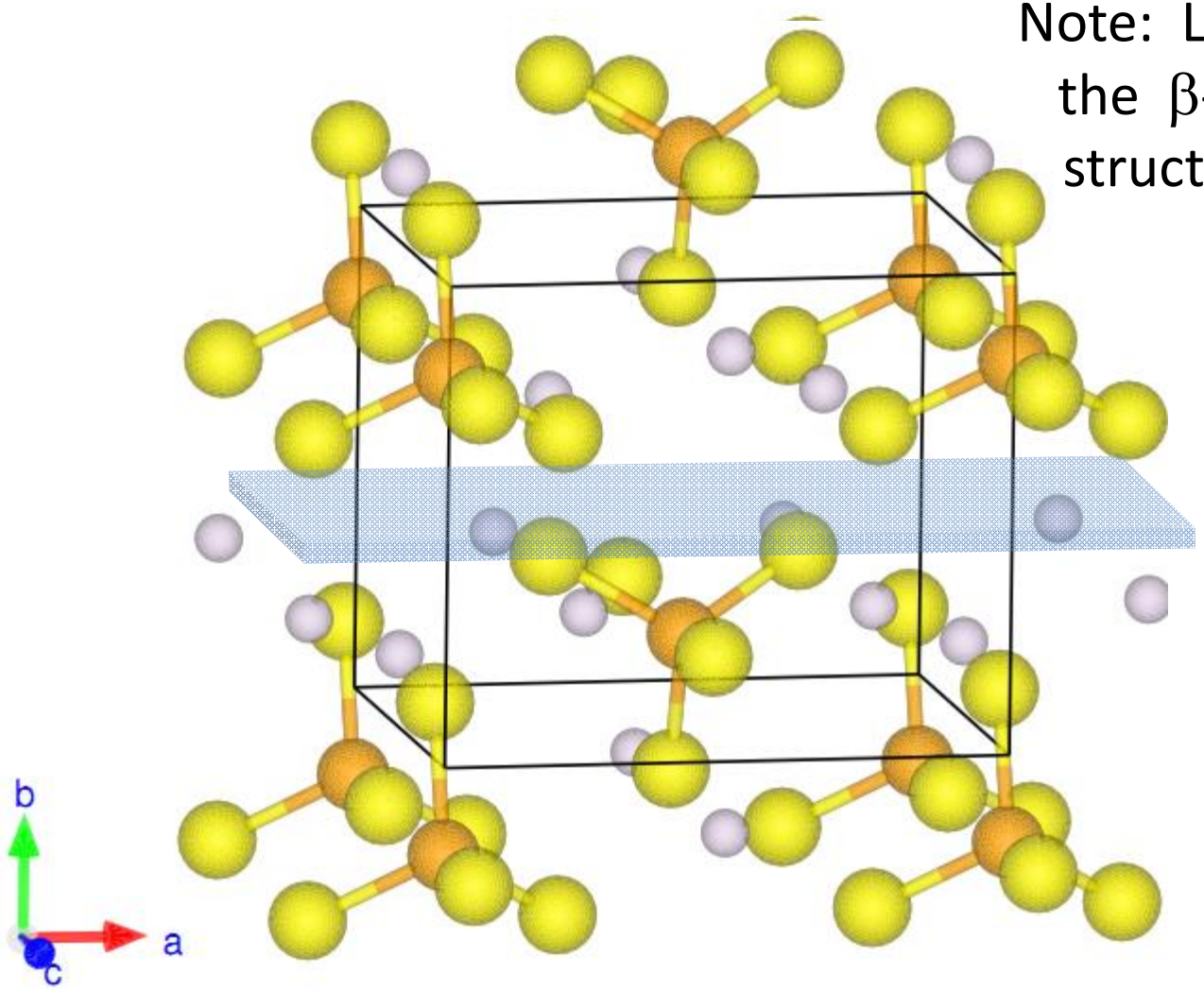

Note: Li_3PS_4 is also found in the β-form with Pnma (#62) structure

Li
N
O
P
S

γ-Li_3PS_4 [0 1 0] surface

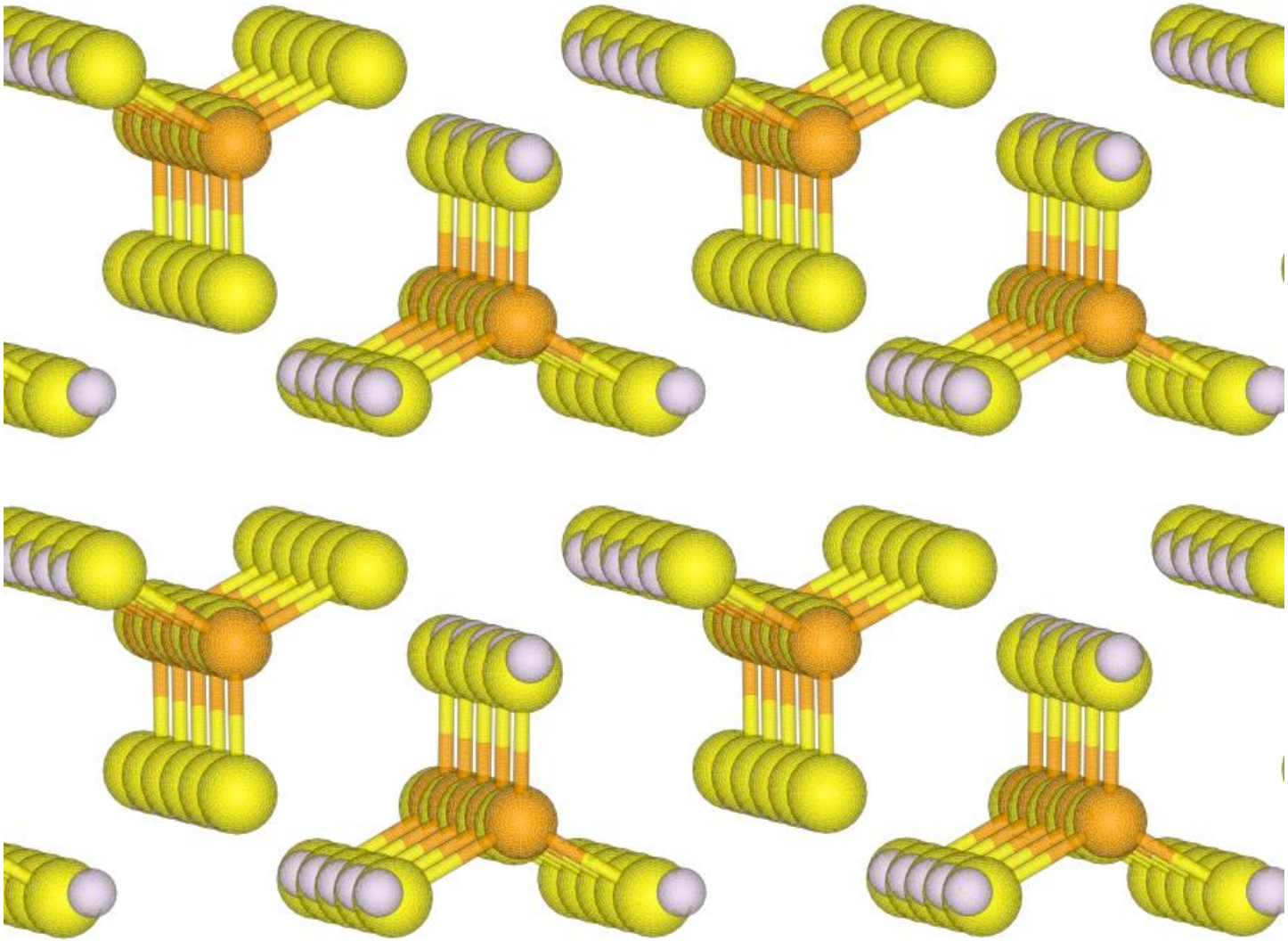

Simulations of ideal γ-Li_3PS_4 [0 1 0] surface in the presence of Li

Initial configuration:

Computed optimized structure:

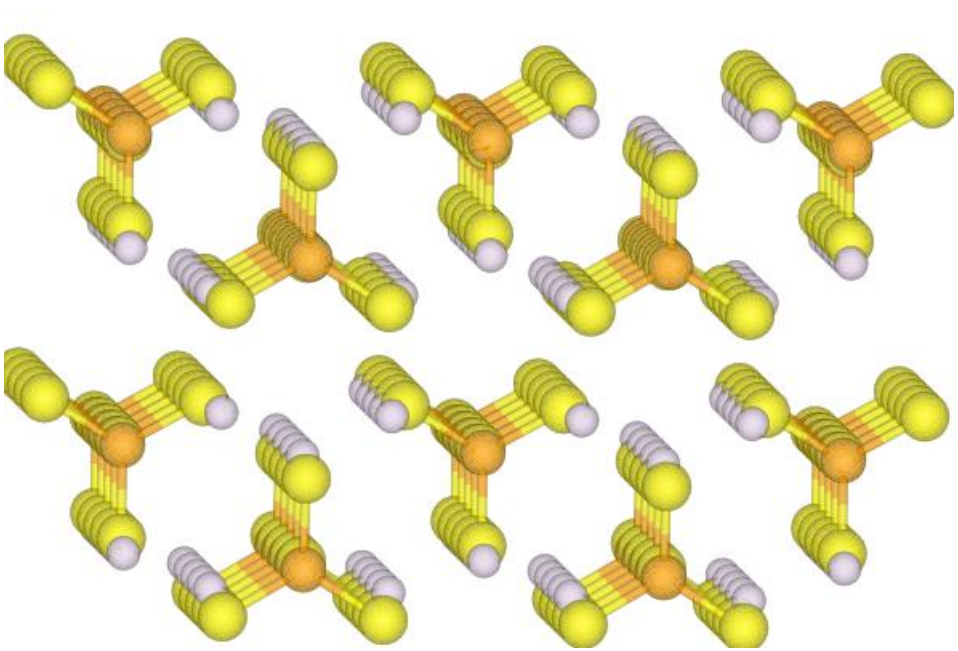

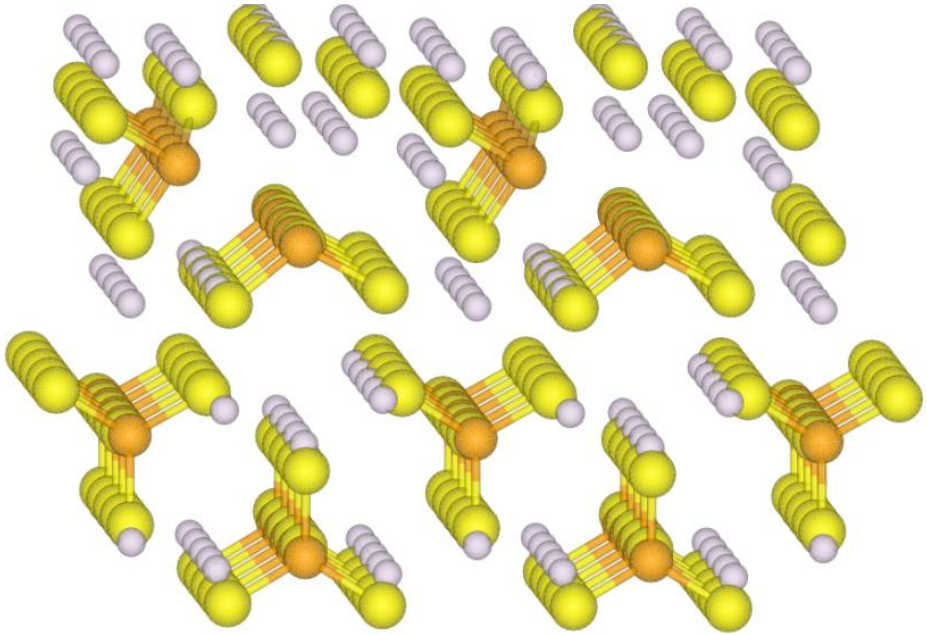

More simulations of ideal γ-Li_3PS_4 [0 1 0] surface in the presence of Li – supercells containing 12 Li atoms and 2 or 4 electrolyte layers

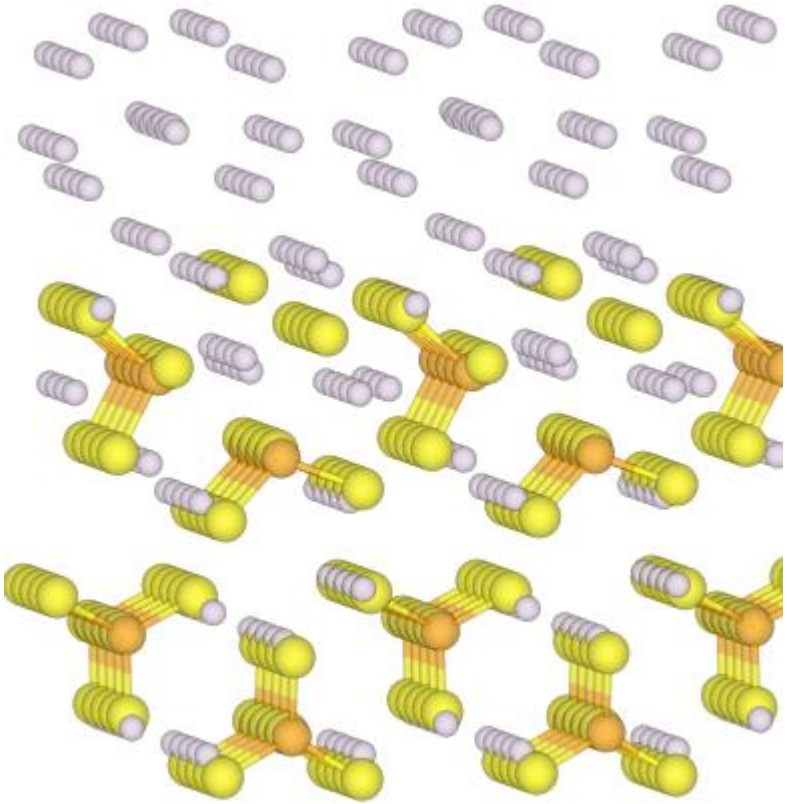

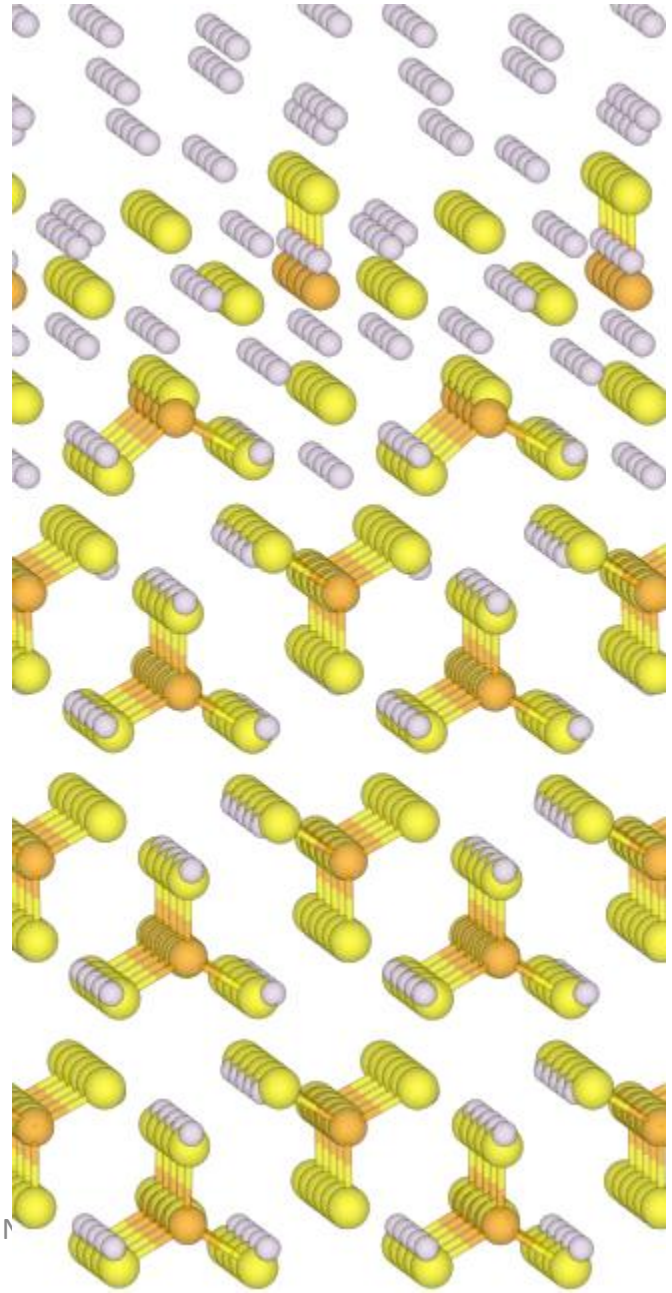

γ-Li_3PS_4 [0 1 0] surface in the presence of Li – supercells containing 12 Li atoms and 2 or 4 electrolyte layers (greater detail)

2 electrolyte layers

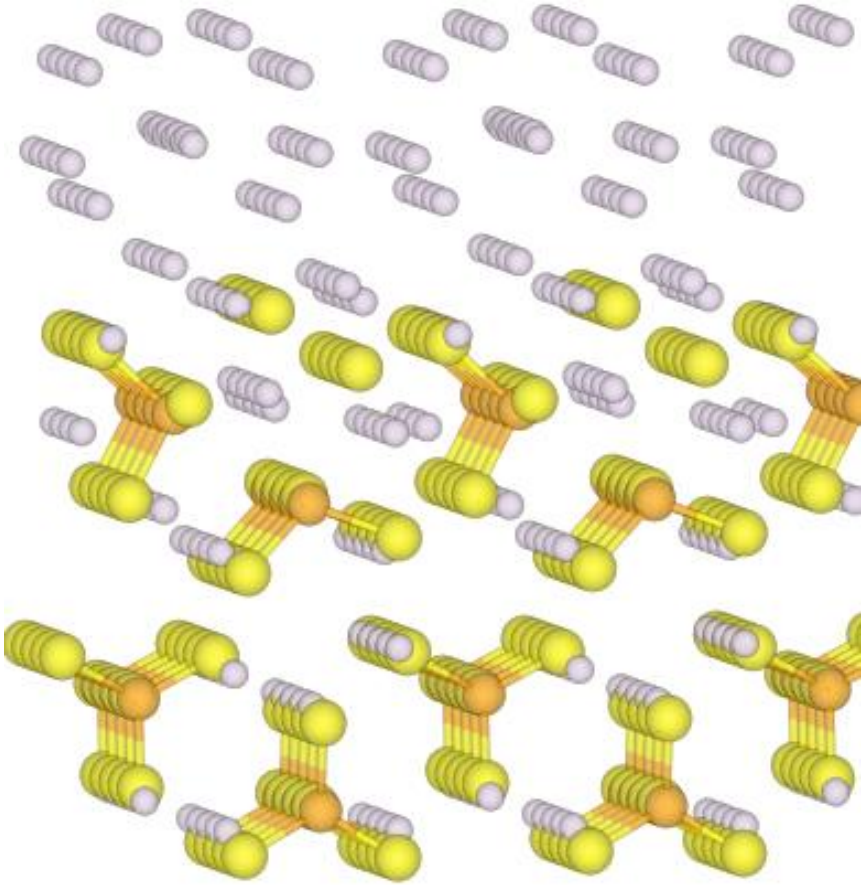

4 electrolyte layers

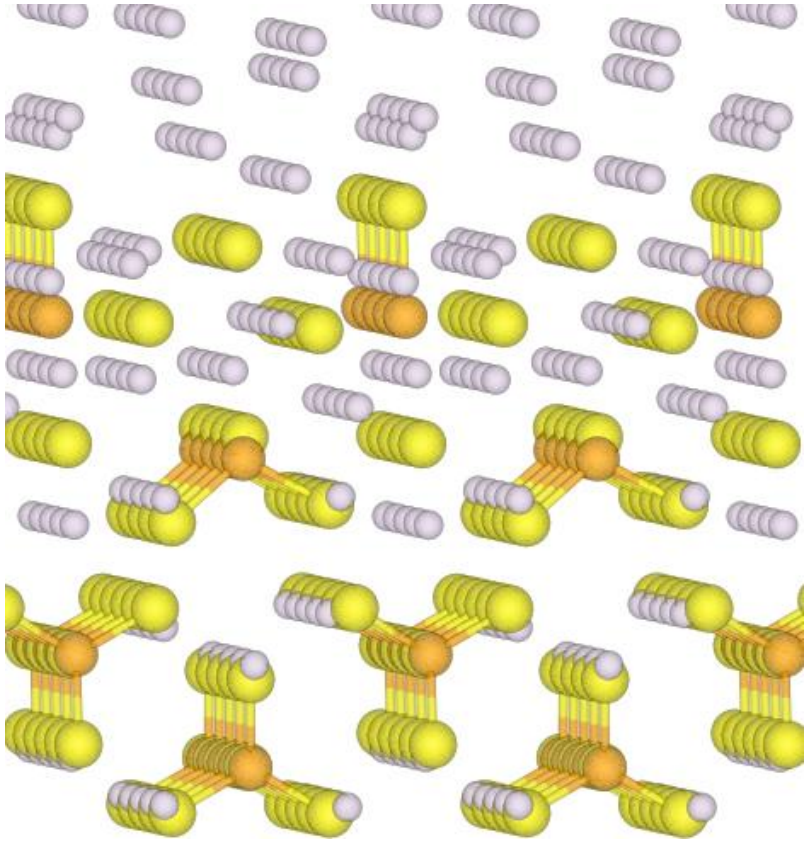

Mystery:

- **Models of ideal Li_3PS_4 surfaces are computational found to be structurally (and chemically) altered by the presence of Li metal. (Also found for β-Li_3PS_4 and for various initial configurations of Li metal.)**
- **Experimentally, the ORNL group has found that solid Li_3PS_4 electrolyte samples can be prepared in Li/ Li_3PS_4/Li cells and cycled many times**

Computational counter example –

stable interface:

Li/β-Li_3PO_4

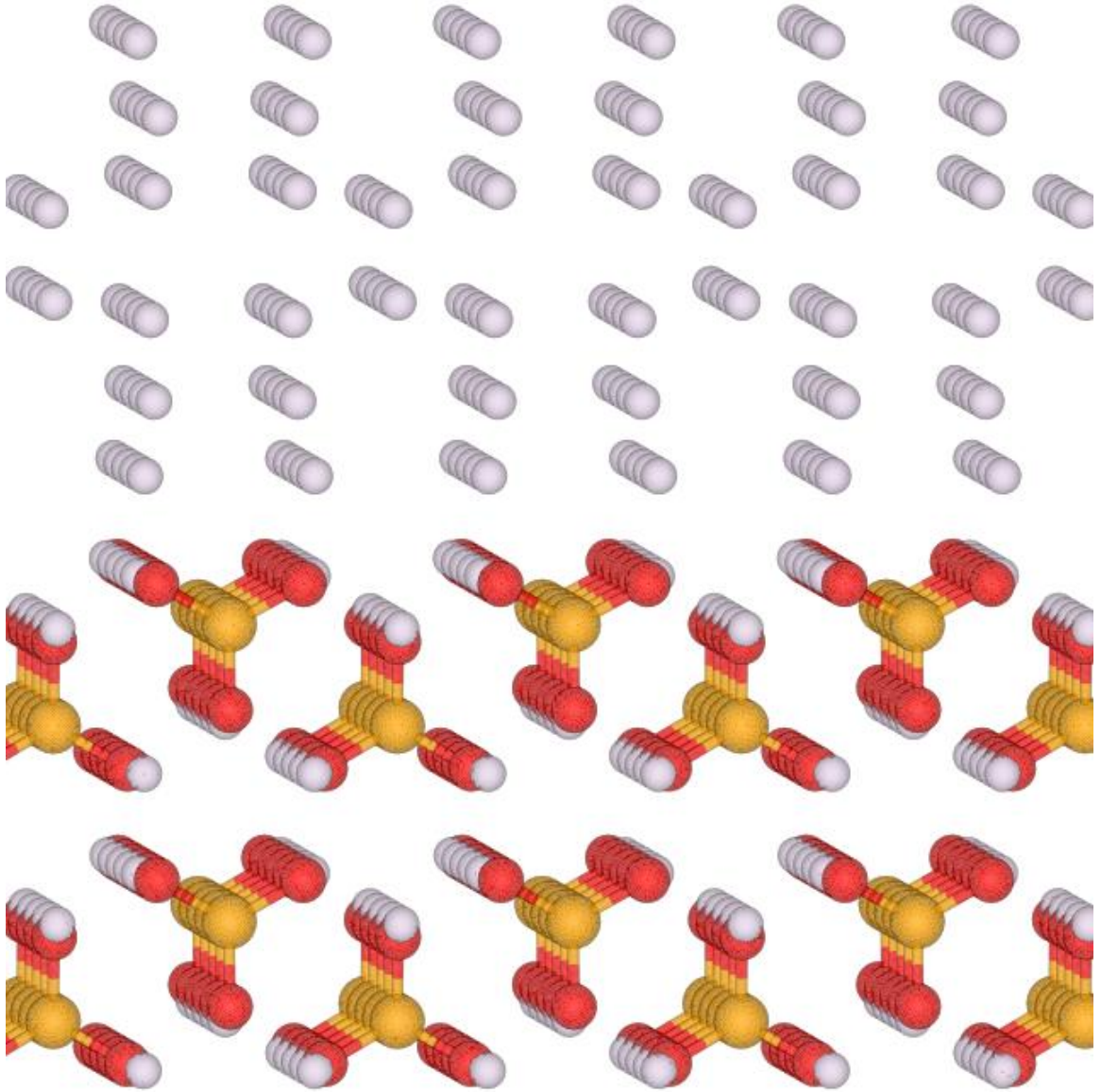

Li

N

O

P

S

Computational counter example – stable interface: Li/*SD*-Li_2PO_2N

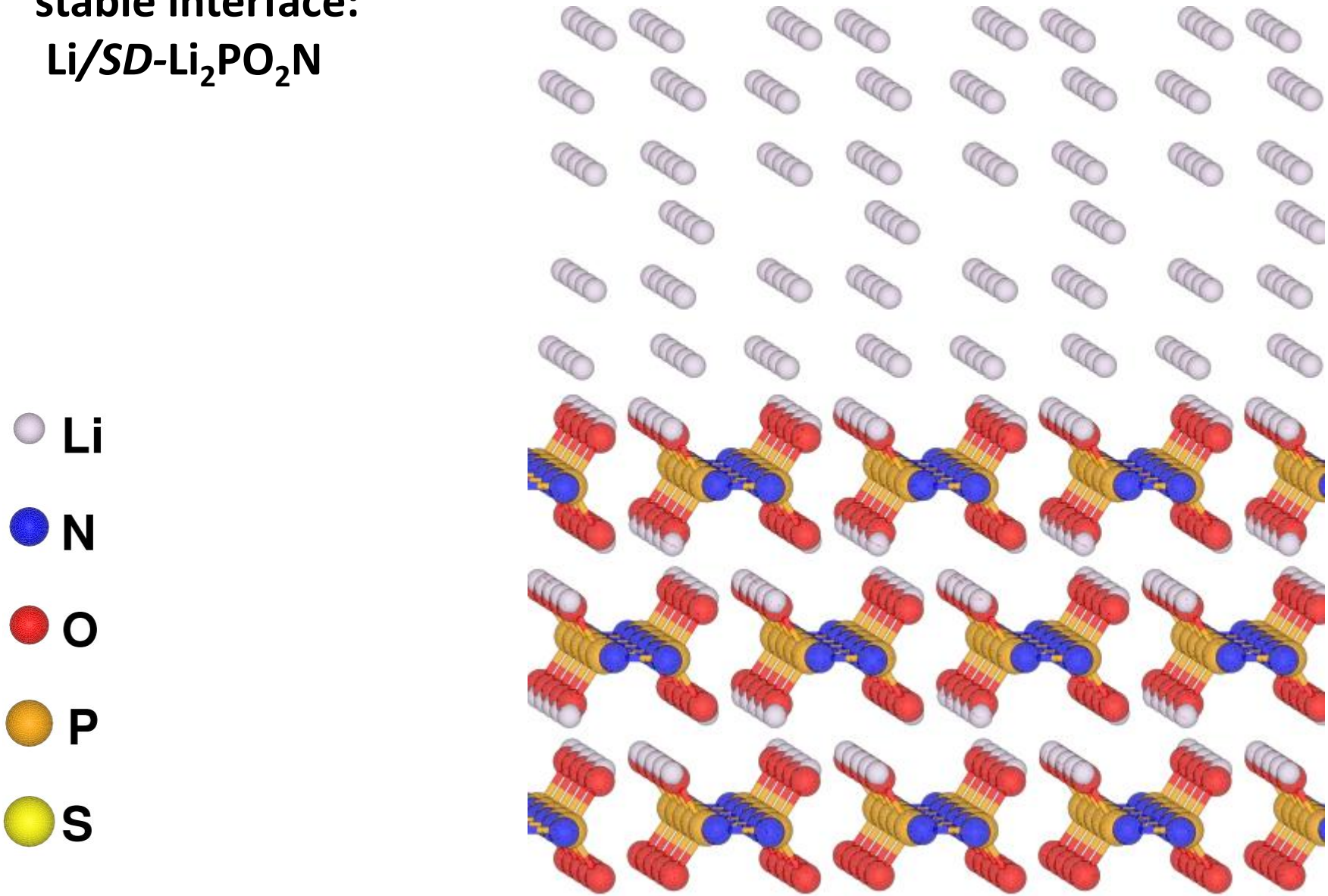

Back to mystery:

- **Models of ideal Li_3PS_4 surfaces are computational found to be structurally (and chemically) altered by the presence of Li metal. (Also found for β-Li_3PS_4 and for various initial configurations of Li metal.)**
- **Experimentally, the ORNL group has found that solid Li_3PS_4 electrolyte samples can be prepared in Li/ Li_3PS_4/Li cells and cycled many times.**

Possible solution:

- **Thin protective buffer layer at Li_3PS_4 surface can stabilize electrolyte – for example $Li_2S/Li_3PS_4/Li_2S$**

Idealized $Li_2S/Li_3PS_4/Li_2S$ system

Details:
Thin film of cubic Li_2S oriented in its non-polar [1 1 0] direction, optimized on [0 1 0] surface of γ-Li_3PS_4. While the Li_2S film was slightly strained, the binding energy of the composite was found to be stable with a binding energy of -0.9 eV.

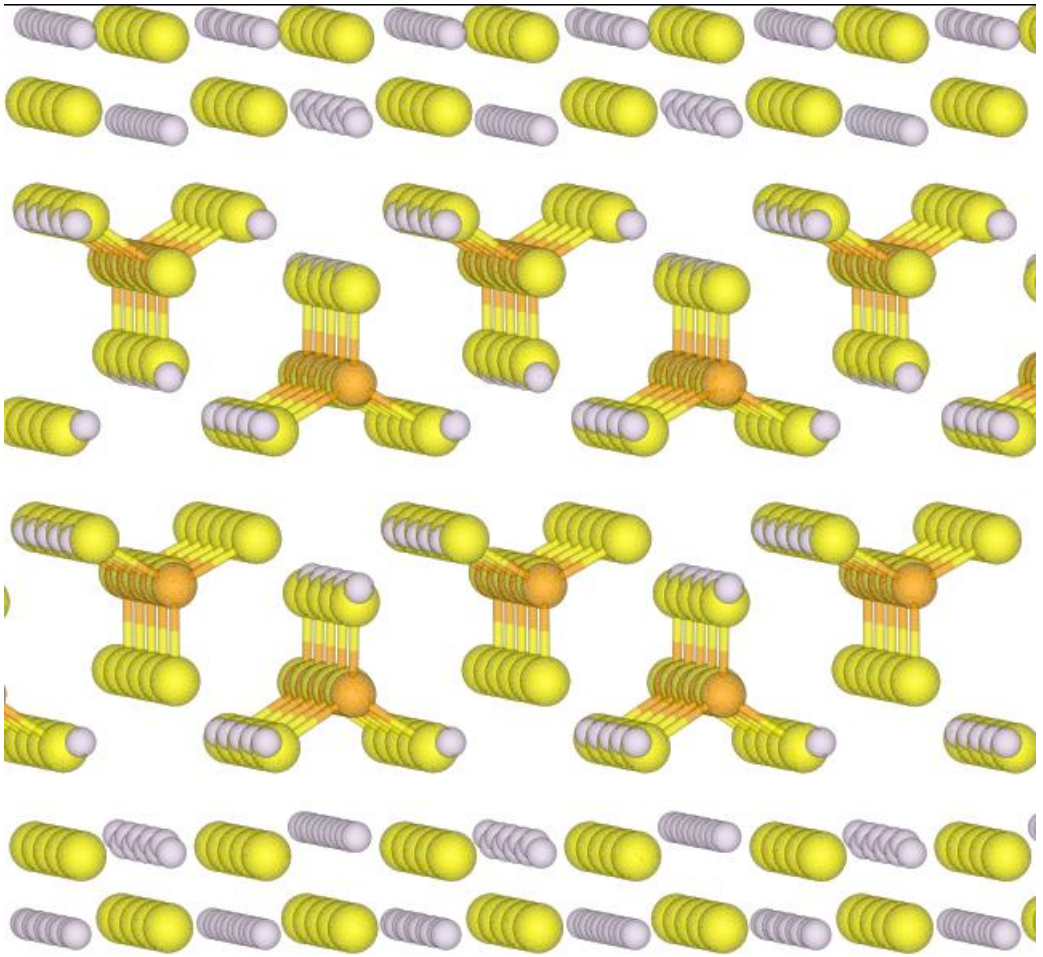

Idealized $Li_2S/Li_3PS_4/Li_2S$ system optimized in presence of Li

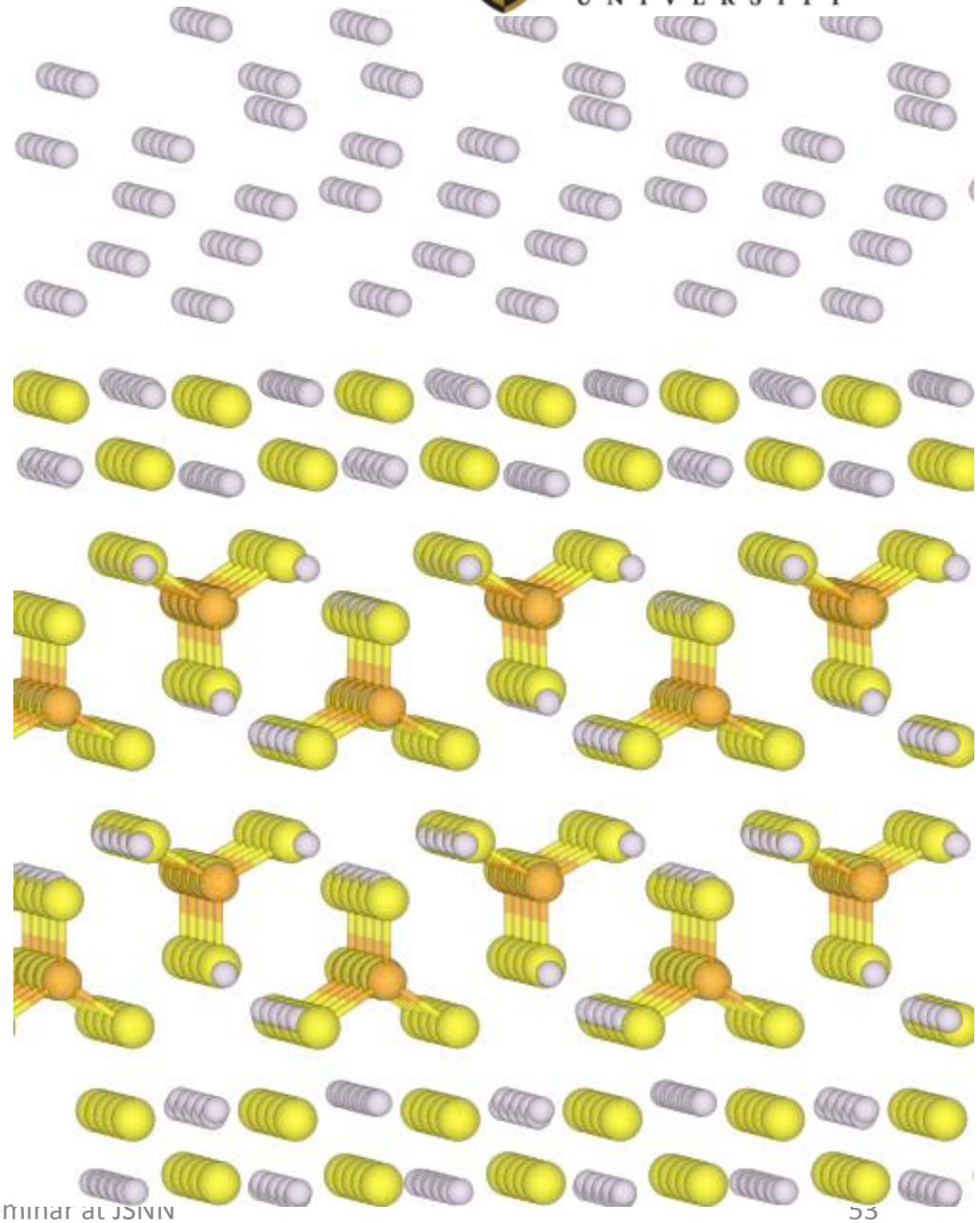

Summary of the interface simulations:

- **Models of ideal Li_3PO_4 and Li_2PO_2N surfaces are computational found to structurally stable in the presence of Li metal.**
- **Models of ideal Li_3PS_4 surfaces are computational found to be structurally (and chemically) altered by the presence of Li metal. (Also found for β-Li_3PS_4 and for various initial configurations of Li metal.)**
- **Thin protective buffer layer of Li_2S at Li_3PS_4 surface can stabilize electrolyte; $Li_2S/Li_3PS_4/Li_2S$ is found to be stable in the presence of Li metal.**
- **Experimentally, the ORNL samples of solid Li_3PS_4 electrolyte, prepared in Li/ Li_3PS_4/Li cells and cycled many times, may form thin buffer layer in first few cycles.**

Additional thoughts

- Limitations of first principles modeling
  - Small simulation cells
  - Zero temperature
- Possible extensions
  - Develop approximation schemes for treatment of larger supercells
  - Use molecular dynamics and/or Monte Carlo techniques
- Ideal research effort in materials includes close collaboration of both simulations and experimental measurements.
- For battery technology, there remain many opportunities for new materials development.